Imperial College London

MSc Dissertation

Imperial College London

Department of Physics

A Review of Loop Quantum Gravity

Author: Hongyi Wan
Supervisor: Prof. João Magueijo

Contents

Abstract

Loop quantum gravity is a proposed theory of quantum gravity that uses connections and holonomies as its fundamental variables, instead of metric variables in Einstein's original formulation of general relativity. LQG proposes a fundamentally discrete picture of spacetime, predicting features such as quantised area and volume, and the resolution of spacetime singularities. In this review, we construct the Hilbert space of LQG, and discuss some of the popular ways dynamics have been defined. In addition, some applications of the theory in black holes and cosmology are discussed.

1 Introduction

Two of the most well established theoretical frameworks in physics are general relativity and quantum field theory. General relativity states that, as opposed to a rigid background, spacetime itself is a dynamic entity, which interacts with the matter that exists within it. Quantum field theory, on the other hand, claims that all elementary particles that we interact with are in fact quantised excitations of fields. Both theories have stood the test of experiments to incredible precision; yet, conceptual problems exist within both of them, suggesting that there is deeper theory that we have not discovered. General relativity, while being incredibly successful at modelling phenomena ranging from the fall of an apple to the expansion of the universe, predicts its own downfall: spacetime singularities inevitably form from the collapse of stars, where curvature becomes infinite. Quantum field theory, on the other hand, is even more severely plagued by infinities. Many expressions only exist as formal expressions, and although some divergences can be removed through renormalisation schemes, we are nonetheless brought to question the true validity of QFT as a fundamental description of nature. On top of that, despite being two of the most precisely tested theories, GR and QFT are constructed from incompatible mathematical frameworks, and therefore cannot be simultaneously true. There are other more subtle issues such as the black hole information paradox, which urges us to revamp our current available theories.

Among many others, two of the most popular candidates of quantum gravity are string theory and loop quantum gravity. String theory postulates that all matter and interactions in the universe manifest from different oscillations of a quantum string, including gravity. It is a subject that covers an immense range of topics, and it is one of the most studied areas in theoretical physics. The other theory, loop quantum gravity, will be the focus of this review. It is a theory that describes a fundamentally discrete spacetime: at the Planck scale of around 10^{-35}m, one reaches the most elementary division of spacetime, and smaller lengths no longer have physical meaning. The conceptual framework of string theory and LQG are drastically different. String theory is proposed to be the description of all phenomena in the universe, while LQG simply constructs a theory of gravity in a quantum framework, with minimal modifications to everything else. In string theory, the curvature of spacetime manifests perturbatively, through propagation of graviton states over a smooth and continuous background. In LQG, the background itself becomes quantised. It is the subject of ongoing debate which of the two theories is the more favourable description of quantum gravity, as both have produced many convincing results, while receiving a fair share of criticism.

The history of LQG can be traced back to the attempts by Wheeler and DeWitt in 1967 [1] to formulate a canonical quantisation of general relativity. This resulted in the Wheeler-DeWitt equation, which is a equation on the wavefunction of the universe. However, numerous conceptual and technical difficulties halted the progress of this program. Ashtekar in 1986 [2] reformulated general relativity in terms of connections and triads in what is known as the Ashtekar variables, which drastically simplified the constraints of GR, making quantisation easier. Around 1990, Rovelli and Smolin began attempting loop quantisation based on the Ashtekar variables, and later introduced spin networks as representations of quantum states of gravity; spin foam formulations of LQG dynamics were also formulated in the 90s. After 2000, numerous people have contributed to the refinement of the theory, in aspects such as the classical limit and the coupling of gravity to matter. Loop quantum gravity remains a continuously developing theory to this day.

We shall begin discussing the theory of loop quantum gravity in the following chapters. In chapter 2, we will go over some foundational aspects of general relativity, which motivates the construction of LQG. In chapter 3, we define the Hilbert space of LQG, and examine its physical interpretations through operator relations. In chapter 4, we discuss some proposed definitions of the dynamics of LQG, going over constructions of time evolution and transition amplitudes. Chapter 5 and 6 will cover applications of the theory in black holes and cosmology. Some important physical constants are: c, the speed of light, $\hbar$, the reduced Plank's constant, and $(8\pi G)$, the gravitational constant. Unless their explicit appearance in equations is important to the discussion, their values will be set to equal 1, using Planck units. We will take the spacetime metric $g_{\mu\nu}$ to have signature $(-1, 1, 1, 1)$.

2 Aspects of General relativity

General relativity, in its original formulation described by the Einstein equations, is a geometric theory of spacetime, in which the dynamic variables are the components of the metric $g_{\mu\nu}$. Over the past century, developments in quantum gravity have shown that the direct quantisation of this theory is difficult. One is therefore motivated to seek alternative formulations of general relativity that facilitate more feasible constructions of a quantum theory of gravity. In this chapter, we will discuss some of the reformulations of Einstein's theory that led to LQG.

2.1 The ADM Formalism

General relativity is a theory symmetric under diffeomorphisms. The Einstein-Hilbert action is invariant under reparameterisations, meaning that spacetime coordinates are arbitrary labels with no physical significance. In quantum mechanics, on the other hand, time is treated very differently from spacial indices, where the dynamics of a system is generated by the Hamiltonian; namely, the Schrodinger equation $i\partial_t |\phi\rangle = H |\phi\rangle$ requires an explicit notion of time. This formulation of quantum dynamics cannot be directly applied to gravity. Because of reparameterisation invariance, the Hamiltonian of general relativity is entirely composed of constraints, leading to the Wheeler-DeWitt equation $H |\phi\rangle = 0$. Instead of describing the dynamics in terms of evolution with respect to a physical time, in general relativity, dynamics is determined by the relation between dynamical variables, described by constraints. Nontheless, to describe gravity in the language of quantum mechanics, one may try to reformulate general relativity using variables that explicitly distinguish time and space, and then attempt to recover spacetime diffeomorphism invariance afterwards. This is the principle behind the Arnowitt-Deser-Misner (ADM) formalism [3]. We will see in chapter 3 that in LQG, Hilbert spaces are defined on spacial slices of spacetime, and the dynamics of the theory is defined by transition amplitudes between two states on spacial slices at different times. The ADM formalism establishes the conceptual foundation for the quantum theory.

We first assume that the topology of a 4-dimensional spacetime is $\mathbb{R} \times \Sigma$, where Σ is a 3-dimensional manifold. To foliate spacetime into spacial slices, one can introduce a fictitious time $t(x)$. The spacial submanifolds are then slices of constant t, denoted Σ_t. Associated with the time function, one also introduces a vector field $t^\mu(x)$, satisfying the condition

$$t^\mu \partial_\mu t = 1. \tag{2.1}$$

This vector field represents the flow of time: beginning with a spacial slice Σ_t, flowing along $t^\mu(x)$ generates translation into subsequent slices. In addition, we also construct a unit length vector field, orthogonal to Σ_t: n^μ such that $n^\mu g_{\mu\nu} n^\nu = -1$. With it, we can decompose t^μ into components, one orthogonal to Σ_t and one tangent to it:

$$t^\mu = N n^\mu + N^\mu. \tag{2.2}$$

This expression produces the two quantities important to the ADM formalism: N, known as "lapse", and N^μ, known as "shift". We can then explicitly choose the function $t(x)$ as the zeroth component of the coordinates, so $x^\mu = (t, x^1, x^2, x^3)$. This is the "time gauge" parameterisation. In this gauge, $N^0 = 0$, so it can be regarded as a vector on Σ_t. On the other hand, the only non-zero component of t^a is t^0. We define the 3-dimensional metric on the spacial submanifolds:

$$q_{ab} = g_{ab} + n_a n_b, \tag{2.3}$$

where a and b range from the spacial indices 1, 2, and 3. The spacetime metric $g_{\mu\nu}$ can then be expressed by the lapse, the shift, and the 3-metric:

$$ds^2 = (-N^2 + q_{ab}N^a N^b)dt^2 + 2q_{ab}N^a dx^b dt + q_{ab}dx^a dx^b. \tag{2.4}$$

We can now analyse the physics using these variables. First, the Einstein-Hilbert action can be rewritten. Omitting some boundary terms, the action can be expressed as

$$\begin{aligned} S &= \int d^4x\sqrt{-g}R(g_{\mu\nu}) \\ &= \int dt \int d^3x N\sqrt{q}(R(q_{ab}) + K_{ab}K^{ab} - K^2). \end{aligned} \tag{2.5}$$

Here we have defined the extrinsic curvature of the spacial manifold:

$$K_{ab} = \frac{1}{2N}(\partial_t q_{ab} - D_{(a}N_{b)}), \tag{2.6}$$

and $K = K_{ab}q^{ab}$. It is important to note that the Einstein-Hilbert action contains second derivatives of the metric. As a result, if we want to study fully the dynamics of the theory, we cannot simply ignore the boundary terms, like it is often done in ordinary field theories. However, for our purposes here, boundary terms do not affect the discussions, so for the sake of keeping the calculations manageable, they will be discarded. From the reformulated action, we can work out the conjugate momenta:

$$\begin{aligned} &\pi^{ab} = \frac{\partial\mathcal{L}}{\partial\dot{q}_{ab}} = \sqrt{q}(K^{ab} - Kq^{ab}) \\ &\pi_N = 0 \\ &\pi_{N^a} = 0. \end{aligned} \tag{2.7}$$

The important observation of the ADM formalism is that the lapse and the shift have no conjugate momenta. They are therefore non-dynamical, and they serve as Lagrange multipliers that define the constraints. In fact, the Hamiltonian, in terms of ADM variables, is entirely constructed from constraints, in the form of Lagrange multipliers:

$$\mathcal{H} = -2N_b D_a \pi^{ab} - N\sqrt{q}R + \frac{N}{\sqrt{q}}(\pi_{ab}\pi^{ab} - \frac{\pi^2}{2}). \tag{2.8}$$

On equations of motion, the Hamiltonian equals zero, and it does not generate dynamics through Poisson brackets like ordinary Hamiltonian mechanics. As discussed before, this indicates that dynamics is formulated through relations between dynamical variables, instead of evolution with respect to a fixed time. We can now work out the constraints defined by the Lagrange multipliers:

$$\begin{aligned} 0 &= \frac{\partial \mathcal{L}}{\partial N} = \sqrt{q}(R + K^2 - K^{ab}K_{ab}) \\ 0 &= \frac{\partial \mathcal{L}}{\partial N^a} = 2\sqrt{q}D_b(K^{ab} - Kq^{ab}). \end{aligned} \tag{2.9}$$

Re-expressed in terms of the metric and its conjugate momentum, these equations define quantities

$$\begin{aligned} C &= -qR + \pi^{ab}\pi_{ab} - \frac{1}{2}\pi^2 \\ C^a &= 2D_b\pi^{ab}, \end{aligned} \tag{2.10}$$

known as the "Hamiltonian constraint" and the "momentum constraint" respectively. Physically, these constraints generate time and space reparameterisations. To see this, we begin with the momentum constraint C^a. It is useful to write it in a smeared form, using an arbitrary vector field $\vec{v}(x)$:

$$\begin{aligned} C_{\vec{v}} &= \int d^3x v^a C_a \\ &= 2\int d^3x v^a q_{ac} D_b \pi^{bc} \\ &= -2\int d^3x q_{ac}\pi^{bc} D_b v^a \\ &= -\int d^3x \pi^{ab}(\mathcal{L}_{\vec{v}} q)_{ab}. \end{aligned} \tag{2.11}$$

Total derivatives were discarded as boundary terms. From the last line above, using the properties of the Lie derivative, we can re-express this quantity as

$$C_{\vec{v}} = \int d^3x q_{ab}(\mathcal{L}_{\vec{v}}\pi)^{ab}, \tag{2.12}$$

where, again, boundary terms are omitted. For an arbitrary function of the metric and its conjugate momentum, we can then calculate the poisson bracket:

$$\begin{aligned}
&\{f(q(y),\pi(y),C_{\vec{v}}[q,\pi]\} \\
&= \int d^3x \left(\frac{\delta f}{\delta q_{ab}(x)}\frac{\delta C_{\vec{v}}}{\delta \pi^{ab}(x)} - \frac{\delta f}{\delta \pi^{ab}(x)}\frac{\delta C_{\vec{v}}}{\delta p_{ab}(x)}\right) \\
&= \int d^3x \delta^{(3)}(y-x)\left(-\frac{\partial f(y)}{\partial q_{ab}}(\mathcal{L}_{\vec{v}}q)_{ab} - \frac{\partial f(y)}{\partial \pi^{ab}}(\mathcal{L}_{\vec{v}}\pi)^{ab}\right) \\
&= -\mathcal{L}_{\vec{v}} f(q(y),\pi(y)).
\end{aligned} \tag{2.13}$$

We can therefore see that $C_{\vec{v}}$ generates spacial diffeomorphisms along the vector field $\vec{v}$. The calculation for the Hamiltonian constraint is more complicated, but one can similarly introduce a smearing using an arbitrary function $g(x)$:

$$C_g = \int d^3x \; g \, C(q,\pi), \tag{2.14}$$

and show that the Hamiltonian constraint is responsible for generating time reparameterisations. Therefore, the set of constraints in the ADM formalism correspond to the requirement that the physics must be invariant under both space and time reparameterisations. We have thus successfully recovered the full spacetime diffeomorphism symmetry of general relativity, using quantities defined on the spacial submanifolds.

One may be tempted to proceed and perform canonical quantisation of this theory, following standard procedures of field theories: promote dynamical variables q_{ab} and π^{ab} to operators, convert Poisson brackets into Dirac commutation relations, and introduce a Hilbert space of states $|\phi\rangle$. The constraints can then be implemented as conditions on physical states in the Hilbert space, for example:

$$\hat{C}\,|\phi\rangle = \hat{C}^a\,|\phi\rangle = 0. \tag{2.15}$$

It is at this point that one runs into issues: the form of the Hamiltonian constraint is non-polynomial, and it is difficult to convert it into an operator expression. For the quantisation, we must therefore seek alternative formulations of general relativity.

2.2 Tetrad Actions and Ashtekar Variables

This section references [4] [5]. For this alternative formulation, we first convert the metric variables $g_{\mu\nu}$ in the Einstein theory to tetrads ${e_\mu}^I$. They are related by $g_{\mu\nu} = {e_\mu}^I {e_\nu}^J \eta_{IJ}$, where upper case Latin letters such as I and J are indices in the internal space, with values 0, 1, 2, 3. The matrix inverse of the tetrads are written as ${e^\mu}_I$, and the determinant of the tetrad is denoted e. Using the tetrad variables, general relativity can be formulated in terms of the tetrad-Palatini action:

$$S[e,\omega] = \int d^4x\, e\, e^{\mu}{}_I e^{\nu}{}_J R_{\mu\nu}{}^{IJ}(\omega) \tag{2.16}$$

Here, the spin connection $\omega_\mu{}^{IJ}$ is treated as an independent variable from the tetrad. The tetrad-Palatini action therefore contains more variables than the Einstein-Hilbert action, where the Christoffel symbol $\Gamma^\mu{}_{\alpha\beta}$ depends explicitly on the metric and its derivatives. However, in the tetrad formalism, if one finds the equation of motion by varying the action with respect to the connection, one will obtain the result that the connection equals the torsion-free metric connection, recovering the same relations between the metric and the connection as the Einstein theory. In addition to diffeomorphism invariance, the tetrad formalism gains an additional Lorentz symmetry on the internal space. The action is invariant under local $SO(3,1)$ transformations $e_\mu{}^I \to \Lambda^I{}_J e_\mu{}^J$. This symmetry will manifest as an additional constraint, as we will see. The tetrad-Palatini action has some advantages over the Einstein-Hilbert action. First, because the connection is independent from the tetrad, some calculations are simplified; more importantly, the tetrad action can be coupled to Fermions, while it is impossible to couple metric variables to spinors. For a spinor field Φ^I, the indices are over the internal space, so its covariant derivative with respect to gravity cannot be defined using the Christoffel symbol, which only contains spacetime indices. Using the spin connection in the tetrad formalism, we can write down the covariant derivative of a spinor field:

$$D_\mu \Phi^I = \partial_\mu \Phi^I + \omega_\mu{}^I{}_J \Phi^J. \tag{2.17}$$

Over the past decades, overwhelming evidence has been produced that suggest the existence of spinors, which indicates that the tetrad formulation may be more fundamental than the metric formulation of general relativity. However, if we attempt to quantise gravity using the tetrad action, we will obtain the same constraint equations as (2.10) that arise in the ADM formalism, so the same problems persist. To progress, we notice that a more general family of theories can be constructed, which are classically equivalent to the tetrad-Palatini theory. This can be done by adding a term to (2.16), resulting in a new action:

$$S[e,\omega] = \int d^4x\, e\, e^{\mu}{}_I e^{\nu}{}_J \left(R_{\mu\nu}{}^{IJ} - \frac{1}{2\gamma} \epsilon^{IJ}{}_{MN} R_{\mu\nu}{}^{MN} \right). \tag{2.18}$$

This action yields the same equations of motion as (2.16). On the equations of motion, the connection becomes torsion free. Due to the symmetry properties of the curvature tensor, the second term of (2.18) then becomes

$$\int d^4x \epsilon^{\mu\nu\alpha\beta} R_{\mu\nu\alpha\beta} = 0, \tag{2.19}$$

and the dynamics of the manifold is described by the original action. The parameter γ is known as the Barbero-Immirzi parameter. In different theories, this parameter can take values as both real and complex numbers. Although this new family of actions do not modify

the classical theory, they will change the relation between quantum operators, and affect the form of the constraint equations. We now study an important choice of $\gamma = -i$, which leads to the original formulation of the Ashtekar variables.

We first define the "self-dual" part of the connection:

$$A_\mu{}^{IJ} = \omega_\mu{}^{IJ} - \frac{i}{2}\epsilon^{IJ}{}_{KL}\omega_\mu{}^{KL}. \tag{2.20}$$

It is called the self-dual connection because it satisfies the following relation:

$$\frac{1}{2}\epsilon^{MN}{}_{IJ}A_\mu{}^{IJ} = iA_\mu{}^{MN}. \tag{2.21}$$

Using this connection, we can write the action (2.18), with the choice $\gamma = -i$, equivalently as:

$$S[e,\omega] = S[e,A] = \int d^4x\, e\, e^\mu{}_I e^\nu{}_J F_{\mu\nu}{}^{IJ} \tag{2.22}$$

where $F_{\mu\nu}{}^{IJ}$ is the curvature of $A_\mu{}^{IJ}$:

$$F_{\mu\nu}{}^{IJ} = \partial_\mu A_\nu{}^{IJ} - \partial_\nu A_\mu{}^{IJ} + GA_\mu{}^I{}_K A_\nu{}^{KJ} - GA_\nu{}^I{}_K A_\mu{}^{KJ}. \tag{2.23}$$

The gravitation constant G is explicitly written to emphasize that, if we regard $A_\mu{}^{IJ}$ as a gauge field with $SO(3,1)$ symmetry, it has a coupling strength G. We now carry out a similar procedure used in the ADM formalism, and foliate spacetime into spacial slices. As before, we introduce a time function $t(x)$ anda vector field t^μ that defines a "flow of time". On the spacial submanifold, this allows us to decompose the tetrad $e^\mu{}_I$ into, again, the lapse function N, the shift vector N^a, and this time, a triad $E^a{}_i E^b{}_j \delta^{ij} = q^{ab}$, where lower case Latin letters such as i and j run over spacial indices 1, 2, 3 on the internal space.

The self-dual property of $A_\mu{}^{IJ}$ conveniently allows us to redefine it on the spacial manifolds. Since the $0i$ components are sufficient to determine the full tensor, we can define the "Ashtekar connection":

$$A_a{}^i = iA_a{}^{0i}. \tag{2.24}$$

The conjugate momentum of the Ashtekar connection is the densitised inverse triad: $\tilde{E}^a_i = \sqrt{q}E^a{}_i$. The Ashtekar connection equates to

$$A_a{}^i = \Gamma_a{}^i - iK_a{}^i, \tag{2.25}$$

where $\Gamma_a{}^i = \epsilon^{ijk}\Gamma_{ajk}$ is the torsionless spin connection of the triad, and $K_a{}^i$ derives from the external curvature: $K_a{}^i = K_{ab}E^{bi}$. Using these variables, one can similarly work out the Hamiltonian and momentum constraints:

$$\begin{aligned} C &= \epsilon_{ijk}F_{ab}{}^i\tilde{E}^{aj}\tilde{E}^{bk} \\ C_a &= F_{ab}{}^i\tilde{E}^b_i, \end{aligned} \tag{2.26}$$

where $F_{ab}{}^i = \partial_{(a}A_{b)}{}^i + \epsilon^i{}_{jk}A_a{}^jA_b{}^k$. Again, these constraints correspond to time and space reparameterisations. In addition, there is a constraint responsible for the internal $SO(3)$ symmetry of the triads, named the "Gauss constraint":

$$G^i = D_a\tilde{E}^{ai}. \tag{2.27}$$

The Gauss constraint also appears in Yang-Mills theories. This parallel between the Ashtekar formalism and gauge theories suggests that gravity can be regarded as a gauge field with additional Hamiltonian and momentum constraints. This motivated the treatment of quantum gravity as a Yang-Mills theory, and as we shall see, the quantisation techniques of LQG borrows ideas from lattice gauge theories, where spacetime becomes descretised. The Ashtekar formulation of gravity is useful for quantisation: as we can see, the form of the Hamiltonian constraint is now polynomial. It therefore becomes easier to implement as a quantum operator.

An important detail has been glanced over: with the choice of $\gamma = -i$, the Ashtekar variables describe a complex theory, while general relativity is defined with real variables. This difference may be reconciled by implementing additional "reality conditions" on the densitised triads:

$$\begin{aligned} &(\tilde{E}^a_i\tilde{E}^{bi})^* = \tilde{E}^a_i\tilde{E}^{bi} \\ &(\epsilon^{ijk}\tilde{E}^{(a}_i D_c(\tilde{E}^{b)}_k\tilde{E}^{c)}_j))^* = (\epsilon^{ijk}\tilde{E}^{(a}_i D_c(\tilde{E}^{b)}_k\tilde{E}^{c)}_j)). \end{aligned} \tag{2.28}$$

The first condition ensures the metric q_{ab} is real. The second condition fixes the Poisson bracket between the metric and the Hamiltonian to be real.

Although the choice of $\gamma = -i$ is a useful and historically popular choice, many results in LQG are obtained under the assumption that γ is real. For an arbitrary γ, the generalised Ashtekar connection is

$$A_a{}^i = \Gamma_a{}^i + \gamma K_a{}^i. \tag{2.29}$$

Its conjugate momentum is still the densitised triad $\tilde{E}^a_i$. However, the poisson bracket is modified to include the parameter γ:

$$\{A_a{}^i(x)\ ,\ \tilde{E}^b_j(y)\} = \gamma\delta^b_a\delta^i_j\delta(x-y). \tag{2.30}$$

Since the tetrad-Palatini action corresponds to the choice $\gamma \to \infty$, this connection could not be defined on the original tetraf-Palatini theory, suggesting that the extension to the original theory results in a distinct theory fundamentally. The Hamiltonian constraint in this theory is expressed as

$$C = \tilde{E}^{aj}\tilde{E}^{bk}\left[\epsilon_{ijk}F_{ab}{}^i - 2(1+\gamma^2)(K_{ja}K_{kb} - K_{jb}K_{ka})\right]. \tag{2.31}$$

One may notice that if we set $\gamma = \pm i$, the second term vanishes, and the Hamiltonian constraint indeed equals the simplified form (2.26) in Ashtekar's original formulation.

We now derive an important relation for LQG. First, we rewrite (2.18) in terms of differential forms, such that $e^I = e^I{}_\mu dx^\mu$, and so on, absorbing the spacetime indices. The action can be expressed as

$$S = \int \left(\epsilon_{IJKL}e^K \wedge e^L + \frac{1}{\gamma}e_I \wedge e_J\right) R^{IJ}. \tag{2.32}$$

We have previously interpreted (2.18) as the action involving the self-dual part of the connection. Written in this form, it is clear that we can also interpret it as an action involving the full connection, but the self-dual part of the area 2-form $\Sigma^{IJ} = e^I \wedge e^J$. This allows us to define a 2-form:

$$B^{IJ} = \epsilon^{IJ}{}_{KL}e^K \wedge e^L + \frac{1}{\gamma}e^{(I} \wedge e^{J)}. \tag{2.33}$$

One may in fact show that this is the conjugate momentum to the connection ω, so it is sometimes called the "momentum two-form". We then decompose it into two parts, which can be defined on the spacial submanifolds:

$$\begin{aligned} K^i &= B^{i0} \\ L^i &= \frac{1}{2}\epsilon^i{}_{jk}B^{jk}. \end{aligned} \tag{2.34}$$

From the self-duality of B^{IJ}, it then follows that

$$\vec{K} = \gamma\vec{L}. \tag{2.35}$$

This is called the "linear simplicity constraint", and it will be crucial to the construction of LQG dynamics.

2.3 Holonomy and Loop Quantisation

Holonomies are an important concept to the development of LQG, as well as the study of gauge theories. The techniques introduced in this section will provide important physical insights, and highlight the historical development of LQG. The outline of this section follows [6].

Consider a gauge field ${A_\mu}^{IJ}$ of some group G, in a manifold. This gauge field functions as a connection that allows us to parallel transport objects along paths in the manifold. Suppose there is a vector $\vec{v} = v^I$ on the internal space at a point p_1 in the manifold, and a curve γ that begin at p_1, and end at some other point p_2. This curve can be parameterised as $x^\mu(t)$, with t ranging between 0 and 1. If $\vec{v}$ is parallel transported along γ, a new vector $\vec{v}_\gamma$ will be produced at p_2. The two vectors are related by a matrix:

$$\vec{v}_\gamma = U_\gamma \cdot \vec{v} \tag{2.36}$$

U_γ is known as the holonomy of γ. It is given by

$$U_\gamma[A] = Pe^{\int_\gamma A} = Pe^{\int_\gamma dx^\mu A_\mu}, \tag{2.37}$$

where P denotes that the exponential is "path ordered", meaning that factors in a product are arranged, from left to right, in the order that they appear along γ. For example,

$$P\left(\int_\gamma A\right)^2 = 2\int_0^1 dt_1 \int_0^{t_1} dt_2 \dot{x}^\mu(t_1) A_\mu(t_1) \dot{x}^\mu(t_2) A_\mu(t_2). \tag{2.38}$$

This is similar to the time ordering that appears in quantum field theory. Since the holonomy is a result of parallel transportation, it is the solution to the differential equation

$$\dot{U}(t) = \dot{x^\mu}(t) A_\mu(t), \tag{2.39}$$

with the choice $t = 1$ and the initial condition $U(0) = \mathbb{1}$. One can check the transformation of a holonomy under a gauge transformation of the connection, and deduce that it only depends on the beginning and end points of the path γ. For a local gauge transformation, in the form:

$$A_\mu \to A'_\mu = \Lambda A_\mu \Lambda^{-1} + (\partial_\mu)\Lambda^{-1}, \tag{2.40}$$

the holonomy transforms as

$$U_\gamma \to \Lambda(x(0))\, U_\gamma\, \Lambda^{-1}(x(1)). \tag{2.41}$$

This transformation property will play a role in defining the Hilbert space of LQG.

An important category of holonomies are theose of closed loops. One can see that for the set of all closed paths beginning and ending at some point p, the holonomies are matrices that form a group, with a multiplication

$$U_{\gamma_1 \circ \gamma_2} = U_{\gamma_1} U_{\gamma_2} \tag{2.42}$$

and an inverse

$$(U_\gamma)^{-1} = U_{\gamma^{-1}}. \tag{2.43}$$

Here, the composition $\gamma_1 \circ \gamma_2$ refers to going around the closed path γ_1 and then γ_2, and the inverse γ^{-1} refers to travelling around the path γ backwards. The group of holonomies is a subgroup of the general linear group, and the exact group depends on the gauge group and the geometry of the manifold. For gravity on an orientable manifold, the holonomy group of the Levi-Civita connection is $SO(3,1)$. Using holonomies of closed paths, we can define "Wilson loops" by taking traces of the holonomies:

$$W_\gamma = Tr(U_\gamma), \tag{2.44}$$

where γ is a closed path. The complex version of Wilson loops is also sometimes used, expressed as

$$W_\gamma = Tr\left(Pe^{i\int_\gamma A}\right). \tag{2.45}$$

From the cyclic property of the trace and the transformation property (2.41), one can deduce that Wilson loops, in both the real and the complex variation, are gauge invariant objects. It can also be shown that Wilson loops do not depend on the base point of a closed path, such that one may choose any point on the path as the beginning and end point. In fact, it suffices to study Wilson loops of closed paths around one point in the manifold. Consider two points p_1 and p_2, connected by a path γ_{12}. A closed path γ_1 beginning and ending at p_1 can be transformed to a closed path around p_2, with $\gamma_2 = \gamma_{12}\gamma_1(\gamma_{12})^{-1}$; in other words, travelling backwards along γ_{12} from p_2 to p_1, around γ_1, and along γ_{12} back to p_2. The Holonomies are related by

$$U_{\gamma_2} = U_{\gamma_{12}} U_{\gamma_1} (U_{\gamma_{12}})^{-1}. \tag{2.46}$$

The cyclicity of the trace then means that the Wilson loops of γ_1 and γ_2 are equivalent.

One may notice that the form of (2.46) is the same as the transformation (2.41). Therefore, by changing the base point of the paths, one can reproduce the effect of a gauge transformation on holonomies of closed paths. In fact, it can be shown that all gauge invariant information about A_μ can be reconstructed using Wilson loops [7]. This motivated the attempt to quantise gravity as a gauge theory using holonomies, resulting in the so-called "loop representation"

of general relativity. To formulate the quantum theory with holonomies, one may attempt to express states $|\Phi\rangle$ in the Hilbert space using basis states $|\{U_\gamma\}\rangle$ labelled by the set of holonomies on all loops γ in a manifold. The "wavefunction of loops" may be expressed as

$$\begin{aligned}\Phi(\gamma) &= \langle\{U_\gamma\}|\Phi\rangle \\ &= \int DA\, \langle\{U_\gamma\}|A\rangle\, \langle A|\Phi\rangle \\ &= \int DA\, \langle\{U_\gamma\}|A\rangle\, \Phi(A),\end{aligned} \tag{2.47}$$

in the second line, a complete basis of states $|A\rangle$ labelled by the configuration of the gauge field was inserted. While conceptually attractive, difficulties arise with loop quantisation. First, the set of all holonomies $\{U_\gamma\}$ contains redundancy when describing gauge invariant information about the gauge field. The states $|\{U_\gamma\}\rangle$ therefore form an over-complete basis. In addition, it is unclear how one may define an inner product between these states, so important physical quantities such as transition amplitudes cannot be calculated. These problems can be mitigated if one considers a truncation of the theory. Consider a finite subset of loops $\{\gamma_i\}$, where $i = 1, \ldots, N$. A functional of the connection $g[A]$ is "cylindrical" if it is a function of holonomies on γ_i, that is:

$$g[A] = G(U_{\gamma_1}[A], \ldots, U_{\gamma_N}[A]). \tag{2.48}$$

If one assumes the quantum states $|\Phi\rangle$ are cylindrical, then one can express it in basis states of holonomies $|\{U_i\}\rangle$ of the paths γ_i. The inner product between a basis state of holonomies and a basis state of the connection can be defined as

$$\langle\{U_i\}|A\rangle = W^*_{\gamma_1}[A] \ldots W^*_{\gamma_N}[A], \tag{2.49}$$

where W_γ is the complex Wilson loop. This allows the conversion between wavefunctionals on the connection to wavefunctions of loops:

$$\Phi(U_i) = \int DA\, W^*_{\gamma_1}[A] \ldots W^*_{\gamma_N}[A] \Phi[A]. \tag{2.50}$$

In addition, one may define the inner product between two states using the loop basis:

$$\langle\Psi|\Phi\rangle = \int_G dU_{\gamma_1} \ldots \int_G dU_{\gamma_N}\, \Psi^*(U_{\gamma_1} \ldots U_{\gamma_N}) \Phi(U_{\gamma_1} \ldots U_{\gamma_N}). \tag{2.51}$$

Where dU_γ is the Haar measure of the group G of holonomies, defined by

$$\int_G dU = 1$$
$$dU = d(gU) = d(Ug) = d(U^{-1}),\ \forall g \in G. \tag{2.52}$$

Since this theory only depends on a finite number of loops, it will not be able to capture the full geometry of the manifold. As we shall see, in LQG, the truncation in degrees of freedom will lead to the interpretation that spacetime is fundamentally discrete.

2.4 Regge Calculus

Regge calculus is one of the early attempts at disctetising general relativity, introduced by Tullio Regge in 1961 [8]. For simplicity, we begin with the discretisation of a 2-dimensional manifold into triangles. The triangles are joined by their edges, and the edges are in turn joined at points. We assume that the internal geometry of each triangle is flat. Therefore, all information about curvature is contained in the geometry at points where the triangles join. This curvature can be approximated through "deficit angles" [9].

Consider a set of triangles Δ_i in the discretisation that are joined at a point p. We use θ_i to label the angle where triangle Δ_i joins at p. This angle can be calculated using the side lengths:

$$cos(\theta_i) = \frac{c^2 - a^2 - b^2}{2ab}. \tag{2.53}$$

Curvature arises if the sum $\sum \theta_i$ differs from 2π. This defines the deficit angle at p:

$$\theta_p(l_s) = 2\pi - \sum_i \theta_i(l_s), \tag{2.54}$$

where l_s refers to the lengths of edges of the triangles. This idea can be generalised to higher dimensions: in 3-dimensions, where a manifold is discretised into tetrahedra, the deficit angle is measured around an edge; in 4-dimensions, a manifold is discretised into 4-simplices, and the deficit angle is measured around a triangle. In general, for a d-dimensional manifold, the deficit angles are measured around the $(d-2)$ dimensional hinges. The remarkable result is that Regge constructed an action using the discretised variables, which approaches the Einstein-Hilbert action in the continuous limit. This action is written as

$$S(l_s) = \sum_h A_h(l_s)\theta_h(l_s). \tag{2.55}$$

the index h sums over all $(d-2)$ dimensional hinges in the discretisation, and A_h is the $(d-2)$ dimensional volume of the hinges. This discretisation provides a possibility of introducing a length scale cut-off, thus providing a regularisation to quantum gravity. However, the Regge

action uses the lengths l_s as its variables, which are subject to the triangle inequality. This results in a highly constrained space of solutions, making quantisation difficult. In the next chapter, we will see that, by switching to a different set of variables after discretisation, quantisation becomes possible.

We have now developed all relevant background theories needed, and in the next chapter, we will begin to define the theory of loop quantum gravity.

3 Kinematics: The States and Operators of LQG

Since Loop quantum gravity is a theory still under development, its formulation continues to evolve, and its physical interpretations adapt accordingly. For this chapter, we will examine the theory defined and interpreted by Rovelli and Vidotto in their writing in [10], as well as Rovelli's lectures in [11]. Rovelli is among the most important contributors to the development of loop quantum gravity, and these sources provide the most up to date formulation of the theory. Where relevant, extended discussion about the theory from other sources will also be studied. In this chapter, the Hilbert space and operators of LQG will be defined.

3.1 Classical Discretisation

We first consider a discretisation of a 3-dimensional manifold Σ that breaks it down into tetrahedra. We then associate a graph Γ to the discretisation, by assigning a node n to each tetrahedra, and a link l to each pair of tetrahedra that share a common face. This graph will be later used to define the Hilbert space of loop quantum gravity. One can view the discretisation as the "dual" to the graph, and denote it with Γ^*; that is, each node in Γ corresponds to a tetrahedron in Γ^*, and each link in Γ corresponds to a traingular face in Γ^*. Because the manifold is discretised using tetrahedra, the nodes in Γ will always be 4-valent, that is, each node connects to 4 links. One may consider discretisations using other shapes, which will result in graphs with different topologies. However, most of the current developments in LQG are achieved using discretisations with tetrahedra, and it is unknown whether graphs of different topologies will result in fundamentally distinct theories.

We now investigate the geometric properties of the discretisation. First, one can define a quantity E_i by integrating the densitised inverse triads $\tilde{E}^a_i$ over a face F of a tetrahedron:

$$E_i = \int_F d\sigma^1 d\sigma^2 n_a \tilde{E}^a_i, \tag{3.1}$$

where σ^1 and σ^2 are the parameterisations of the face F, and $n_a = \epsilon_{abc}\frac{\partial x^b}{\partial \sigma^1}\frac{\partial x^c}{\partial \sigma^2}$ is a vector normal to F. By inspecting this integral expression, one can see that E_i represents the flux of $\tilde{E}^a_i$ through F. However, there is a more geometrical interpretation: assuming the metric is constant inside the tetrahedron, one can fix parameterisation and gauge of the triads so that $\tilde{E}^a_i = \delta^a_i$. The components E_i then form a vector $\vec{E}$, whose direction is normal to F, and whose magnitude is the area of F. This interpretation becomes clear if one considers that E_i can be equivalently expressed as the integration over F of the area 2-form:

$$E_i = \frac{1}{2}\epsilon_{ijk}\int_F e^j \wedge e^k. \tag{3.2}$$

By considering the geometry of a tetrahedron, one will find the "closure" relation: denote the normal vector associated with each face of the tetrahedron as $\vec{E}_1$, ..., $\vec{E}_4$, then

$$\vec{E}_1 + \vec{E}_2 + \vec{E}_3 + \vec{E}_4 = 0. \tag{3.3}$$

The volume of a tetrahedron can also be expressed using the vectors $\vec{E}$ as:

$$V^2 = \frac{2}{9} \left| \epsilon^{ijk} (E_1)_i (E_2)_j (E_3)_k \right|. \tag{3.4}$$

Because of the closure relation, one may choose any 3 faces of the tetrahedron, and find the same value for V^2.

In addition, one can calculate the dihedral angle θ between two faces:

$$\left|\vec{E}_1\right| \left|\vec{E}_2\right| sin(\theta) = \vec{E}_1 \cdot \vec{E}_2. \tag{3.5}$$

3.2 The Hilbert Space of Loop Quantum Gravity

We now define the Hilbert space of the theory. On the manifold Σ, we define a generalised Ashtekar connection $A_a{}^i$, given in (2.29). For a graph Γ embedded in Σ, the embedding of a link l_i in Σ can be regarded as a path γ_i in the manifold. One can then define a holonomy associated with each link:

$$U_i = P e^{\int_{\gamma_i} A_a{}^i T_i}, \tag{3.6}$$

where $T_i = -\frac{i}{2}\sigma_i$ are the generators of the $su(2)$ algebra, which is isomorphic to the algebra $so(3)$ (here σ_i denote the Pauli matrices). As a result, the holonomies will take values in the group $SU(2)$, which is the double cover of $SO(3)$. Given a gauge transformation of the connection (2.40) parameterised by $\Lambda(x)$, it follows from (2.41) that the holonomies transform as

$$U_i \to \Lambda_{s_i} \, U_i \, \Lambda_{t_i}^{-1}, \tag{3.7}$$

where Λ_{s_i} and Λ_{t_i} respectively refer to the gauge transformation at the source node and the target node of the link. For a graph Γ with p links and q nodes, the states in LQG are the set of square-integrable wavefunctions on the p holonomies, written as $\Psi(U_i)$. (Note that, for a graph that contains only 4-valent nodes, i.e. those associated with discretisations using tetrahedra, one will obtain the relation $p = 2q$. However, as previously discussed, theories in LQG can be constructed by considering discretisations with other shapes, so for more generality, we will consider a wider class of graphs, where p and q are unrelated.) The inner product defined on these states takes the form of (2.51), where the integration variable dU_i is the Haar measure of $SU(2)$. The Hilbert space is the collection of such wavefunctions, denoted as

$$\mathcal{H} = L^2[SU(2)^p]. \tag{3.8}$$

This Hilbert space is independent from the topology of the graph Γ, since the wavefunctions $\Psi(U_i)$ do not contain information on how the links are joined at the nodes; only the number of links p is relevant.

The Hilbert space formulated this way contains unphysical states, since not all wavefunctions in $L^2[SU(2)^p]$ satisfy the quantum versions of the constraint equations that define the dynamics of general relativity. We first impose the Gauss constraint (2.27), which corresponds to the condition that physical states must be invariant under gauge transformations. Suppose there is an operator that produces gauge transformations, denoted $\mathcal{U}[\Lambda]$. Its action on a wavefunction is

$$\mathcal{U}[\Lambda]\Psi(U_i) = \Psi(\Lambda_{s_i}\, U_i\, \Lambda_{t_i}^{-1}). \tag{3.9}$$

Then a gauge invariant wavefunction must satisfy $\mathcal{U}[\Lambda]\Psi(U_i) = \Psi(U_i)$, for any choice of gauge transformation at the q nodes. This set of physical states form a subspace of the Hilbert space (3.8), written as

$$\mathcal{H}_\Gamma = L^2[SU(2)^p/SU(2)^q]_\Gamma \tag{3.10}$$

that is, the subspace of (3.8), invariant under q $SU(2)$ gauge transformations. The subscript Γ emphasizes that the states now depend on the topology of Γ: the holonomies of links joined at the same node will transform under the same local gauge transformation. The Hilbert space (3.10) defined above will describe the quantum states of loop quantum gravity satisfying the Gauss constraint. However, it is often simpler to perform calculations on the larger space of states (3.8), so it will also be utilised in the following sections.

3.3 Spin Networks

We now construct a set of basis states in the Hilbert space (3.8), and following that, a set of basis states for the gauge invariant subspace $\mathcal{H}_\Gamma$, in the form of spin networks.

First, we introduce the Wigner matrices: a Wigner matrix $D^j_{ab}(g)$, where $g \in SU(2)$, is an element in the spin-j representation of $SU(2)$. Its elements can be computed by considering rotations of spin-j basis states:

$$D^j_{mn}(g) = < j, m|\hat{R}(g)|j, n >, \tag{3.11}$$

where $\hat{R}(g)$ is the rotation operator:

$$\hat{R}(G) = \hat{R}(\alpha, \beta, \gamma) = e^{-i\alpha\hat{J}_z} e^{-i\beta\hat{J}_y} e^{-i\gamma\hat{J}_x}, \tag{3.12}$$

where α, β, γ are the Euler angles associated with the group element g.

Consider a function $f(g) \in L^2[SU(2)]$ on one $SU(2)$ group element g. The Peter-Weyl theorem states that the elements of the Wigner matrices $D^j_{ab}(g)$ form a complete orthogonal basis for $L^2[SU(2)]$. That is, they satisfy the equations of orthogonalty:

$$\int_{SU(2)} dg D^i_{ab}(g) D^j_{cd}(g) = \frac{1}{2j+1} \delta^{ij} \delta_{ac} \delta_{bd} \tag{3.13}$$

and completeness:

$$\delta(g_1 g_2^{-1}) = \sum_j (2j+1) D^j_{ab}(g_1) D^j_{ba}(g_2^{-1}). \tag{3.14}$$

Thus, any square integrable function $f(g)$ can be decomposed into elements of the Wigner matrices:

$$f(g) = \sum_j f^{ab}_j \, \phi^j_{ab}(g), \tag{3.15}$$

where $\phi^j_{ab} = \sqrt{2j+1}\, D^j_{ab}$ are the normalised matrix elements, and

$$f^{ab}_j = \int_{SU(2)} dg \, \phi^j_{ab}(g^{-1}) \, f(g). \tag{3.16}$$

Similarly, wavefunctions in $L^2[SU(2)^p]$ can be decomposed into products of elements of Wigner matrices:

$$\Psi(U_1, ..., U_p) = \sum_{j_1, ..., j_p} \Psi^{a_1 ... a_p, \, b_1 ... b_p}_{j_1 ... j_p} \, \phi^{j_1}_{a_1 b_1}(U_1) \, ... \, \phi^{j_p}_{a_p b_p}(U_p). \tag{3.17}$$

Thus, one can express any state in the Hilbert space in a basis of wavefunctions

$$\prod_{i=1}^{p} \phi^{j_i}_{a_i b_i}(U_i). \tag{3.18}$$

We now find the set of gauge invariant states. In the graph Γ, consider a set of r links joined at the same node n. Since the labelling of links and the assignment of their direction are physically irrelevant, for simplicity we assign the r links with indices 1, ..., r, and they all have n as their source node. A wavefunction on this graph can be written as

$$\Psi(U_1, ..., U_p) = \sum_{j_1, \, ..., \, j_r} F^{a_1 ... a_r, \, b_1 ... b_r}_{j_1 ... j_r}(U_{r+1}, ..., U_p) \, \phi^{j_1}_{a_1 b_1}(U_1) \, ... \, \phi^{j_r}_{a_r b_r}(U_r). \tag{3.19}$$

Here the tensor F contains all information about the wavefunction related to the rest of the links. Consider now a gauge transformation Λ at the node n. The basis elements $\phi^{j_i}_{a_i b_i}$, with $i = 1, ..., r$, transform as

$$\phi^{j_i}_{a_i b_i}(U_i) \to \phi^{j_i}_{a_i b_i}(\Lambda U_i) = D^{j_i}_{a_i c_i}(\Lambda)\phi^{j_i}_{c_i b_i}(U_i). \tag{3.20}$$

Thus, to find the set of gauge invariant wavefunctions $\Psi(U_i)$ corresponds to the requirement that the tensor F is invariant under transformations

$$F^{a_1 ... a_r,\, b_1 ... b_r}_{j_1 ... j_r} = D^{j_1}_{a_1 c_1}(\Lambda)...D^{j_r}_{a_r c_r}(\Lambda)F^{c_1 ... c_r,\, b_1 ... b_r}_{j_1 ... j_r}. \tag{3.21}$$

Such tensors are known as "intertwiners". For a trivalent node, that is, a node which joins 3 links, given the spins that label the Wigner matrices associated with the 3 links, there is a unique tensor $i^{a_1 a_2 a_3}$, up to normalisation, that is invariant under gauge transformations. This tensor is expressed by the "Wigner 3j symbol":

$$i^{a_1 a_2 a_3} = \begin{pmatrix} j_1 & j_2 & j_3 \\ a_1 & a_2 & a_3 \end{pmatrix}. \tag{3.22}$$

For the Wigner 3j symbols to have non-zero values, the spins j_1, j_2, j_3 must satisfy the following conditions:

$$\begin{aligned} &j_1 + j_2 + j_3 \in \mathbb{N} \\ &|j_1 - j_2| \leqslant j_3 \leqslant j_1 + j_2, \end{aligned} \tag{3.23}$$

that is, they must sum to an integer, and they satisfy the triangle inequalities. In addition, the Wigner 3j symbol $i^{a_1 a_2 a_3}$ is only non-zero if $a_1 + a_2 + a_3 = 0$. For nodes that join more than 3 links, the intertwiners $i^{\,a_1 \,\cdots\, a_N}$ can be constructed by contracting multiple Wigner 3j-symbols. This corresponds to decomposing a node into multiple trivalent nodes, joined by virtual links. For 4-valent nodes, an intertwiner with 4 indices can be calculated from the contraction of 2 Wigner 3j-symbols:

$$i_k{}^{a_1 a_2 a_3 a_4} = \begin{pmatrix} j_1 & j_2 & k \\ a_1 & a_2 & b \end{pmatrix} \delta_{bc} \begin{pmatrix} k & j_3 & j_4 \\ c & a_3 & a_4 \end{pmatrix}. \tag{3.24}$$

There is therefore a family of 4-valent intertwiners, labelled by the spin of the virtual link k.

Therefore, a gauge invariant wavefunction can be written as a product of intertwiners associated with each node, and Wigner matrices associated with each link, for instance:

$$\Psi(U_1, ..., U_p) = \sum_{j_1, \,..., \,j_p} K\, i^{\,a_1 \,\cdots\, a_k} ... \, i^{\,a_{(p-l)} \,\cdots\, a_p}\, i^{\,b_1 \,\cdots\, b_m} ... \, i^{\,b_{(p-n)} \,\cdots\, b_p}\, \phi^{j_1}_{a_1 b_1}(U_1) ... \, \phi^{j_p}_{a_p b_p}(U_p), \tag{3.25}$$

where K is a constant of normalisation. This set of states can be graphically represented by spin networks: one assigns a normalised representation matrix $\phi^{j_i}(U_i)$ of spin j_i to each link l_i, and an intertwiner $i^{a_1 \cdots a_N}$ to each node n.

Figure 3.1: Example of a spin network. The numbers label the spins assigned to each link. The intertwiners are not labelled. Figure sourced from [12].

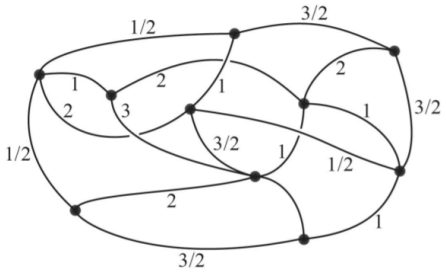

3.4 Geometric Operators

In this section, we discuss some of the operators that act on the Hilbert space $\mathcal{H}_\Gamma$, and from their properties, we will find the physical interpretation of the geometry of LQG.

Consider first the much simpler theory of particle quantum mechanics, where states in the Hilbert space can be represented by wavefunctions $\Psi(x)$. In this theory, we promote classical variables of position x and momentum p to operators, where their Poisson bracket relations become commutation relations

$$\{x, p\} = 1 \rightarrow [\hat{x}, \hat{p}] = i\hbar. \tag{3.26}$$

The actions of these operators on wavefunctions are

$$\begin{aligned} \hat{x}\Psi(x) &= x\Psi(x) \\ \hat{p}\Psi(x) &= -i\hbar\frac{d}{dx}\Psi(x). \end{aligned} \tag{3.27}$$

For LQG, we wish to find an analogous set of operators that act on wavefunctions $\Psi(U_i)$. It is simple to define one half of them: one promotes the configuration variables, which are matrix elements of the holonomy $(U_r)_{ij}$, into operators $(\hat{U}_r)_{ij}$, with their action on wavefunctions simply defined as a multiplication:

$$(\hat{U}_r)_{ij}\Psi(..., U_r, ...) = (U_r)_{ij}\Psi(..., U_r, ...). \tag{3.28}$$

To find the conjugare operator to $(\hat{U}_r)_{ij}$, analogous to $\hat{p}$ in particle QM, recall the generalised Ashtekar variables that LQG is based on. As discussed in previous sections, the theory

defined by the action (2.18) uses the generalised Ashtekar connection ${A_a}^i$ as its configuration variable, while the densitised inverse triad $\tilde{E}^a_i$ acts as the conjugate momentum, with a Poisson bracket

$$\{{A_a}^i(x)\ ,\ \tilde{E}^b_j(y)\} = \gamma\delta^b_a\delta^i_j\delta(x-y). \tag{3.29}$$

Returning to the theory of LQG defined on a graph Γ, we may notice that the holonimies U_r can be regarded as a smearing of the connection ${A_a}^i(x)$ along the embedding of a link l_r. Thus, to reproduce the Ashtekar theory in the continuum limit, one should seek a conjugate operator constructed from the smearing of $\tilde{E}^b_j(y)$. An appropriate candidate to promote into an operator is the quantity E_i, defined in (3.1) by smearing $\tilde{E}^b_j(y)$ over a face F. Recalling that each link l_r is dual to a face F_r, we define a set of operators $(\hat{E}_r)_i$ associated with each link l_r, whose action on wavefunctions is defined as

$$(\hat{E}_r)_i\Psi = \gamma(\hat{L}_r)_i\Psi \tag{3.30}$$

where $(\hat{L}_r)_i$ is a derivative operator on wavefunctions, whose action is defined as

$$\begin{aligned}(\hat{L}_r)_i\Psi(...,U_r,...) &= -i\frac{d}{dt}\Psi(...,U_re^{tT_i},...)|_{t=0}\\ &= -i\lim_{t\to 0}\left[\Psi(...,U_re^{tT_i},...)-\Psi(...,U_r,...)\right],\end{aligned} \tag{3.31}$$

T_i being generators of the $su(2)$ algebra. One can check that the operators satisfy the commutation relation

$$\left[(\hat{U}_r)_{mn},(\hat{L}_s)_i\right] = \delta_{rs}(U_r)_{ml}(T_i)_{ln}. \tag{3.32}$$

We now inspect the properties of the derivative operators $(\hat{L}_r)_i$. Consider a gauge invariant state $\Psi \in \mathcal{H}_\Gamma$. We choose 4 links that share the same target node n_0. Without loss of generality, we again assign indices l_1, ..., l_4 to the links. The relevant part of Ψ can be written, as before:

$$\Psi = \sum_{j_1,\,...,\,j_4} F^{a_1...a_4,\,b_1...b_4}_{j_1...j_4}\ \phi^{j_1}_{a_1b_1}(U_1)\ ...\ \phi^{j_4}_{a_4b_4}(U_4). \tag{3.33}$$

Consider an infinitesimal gauge transformation $\Lambda = \mathbb{1}+t\lambda$ at the node n_0. The wavefunction will transform as

$$
\begin{aligned}
\Psi \to \Psi' &= \sum_{j_1,\,...,\,j_4} F^{a_1...a_4,\,b_1...b_4}_{j_1...j_4}\ \phi^{j_1}_{a_1b_1}(U_1\Lambda)\ ...\ \phi^{j_4}_{a_4b_4}(U_4\Lambda) \\
&= \sum_{j_1,\,...,\,j_4} F^{a_1...a_4,\,b_1...b_4}_{j_1...j_4}\ \phi^{j_1}_{a_1c_1}(U_1) D^{j_1}_{c_1b_1}(\Lambda)\ ...\ \phi^{j_4}_{a_4c_4}(U_4) D^{j_4}_{c_4b_4}(\Lambda) \\
&= \sum_{j_1,\,...,\,j_4} F^{a_1...a_4,\,b_1...b_4}_{j_1...j_4}\ \phi^{j_1}_{a_1c_1}(U_1) \left(\mathbb{1} + td^{j_1}(\lambda)\right)_{c_1b_1}\ ...\ \phi^{j_4}_{a_4c_4}(U_4) \left(\mathbb{1} + td^{j_4}(\lambda)\right)_{c_4b_4},
\end{aligned}
\tag{3.34}
$$

where d^j are spin j representation matrices of $su(2)$ algebra elements. Now consider the operation

$$
\begin{aligned}
&\left[(\hat{L}_1)_i + (\hat{L}_2)_i + (\hat{L}_3)_i + (\hat{L}_4)_i\right]\Psi \\
&= \sum_{j_1,\,...,\,j_4} F^{a_1...a_4,\,b_1...b_4}_{j_1...j_4}\ (-i)[\frac{d}{dt}\phi^{j_1}_{a_1b_1}(U_1e^{tT_i})\ ...\ \phi^{j_4}_{a_4b_4}(U_4) + ... \\
&\quad + \phi^{j_1}_{a_1b_1}(U_1)\ ...\ \frac{d}{dt}\phi^{j_4}_{a_4b_4}(U_4e^{tT_i})]_{t=0} \\
&= \sum_{j_1,\,...,\,j_4} F^{a_1...a_4,\,b_1...b_4}_{j_1...j_4}\ (-i)[\phi^{j_1}_{a_1c_1}(U_1)d^{j_1}(T_i)_{c_1b_1}\ ...\ \phi^{j_4}_{a_4b_4}(U_4) + ... \\
&\quad + \phi^{j_1}_{a_1b_1}(U_1)\ ...\ \phi^{j_4}_{a_4c_4}(U_4)d^{j_4}(T_i)_{c_4b_4}].
\end{aligned}
\tag{3.35}
$$

By inspecting the expressions (3.34) and (3.35), one can see that to for the wavefunction to be gauge invariant $\Psi = \Psi'$, it must satisfy the condition

$$
\left[\vec{\hat{L}}_1 + \vec{\hat{L}}_2 + \vec{\hat{L}}_3 + \vec{\hat{L}}_4\right]\Psi = 0. \tag{3.36}
$$

This property of $\vec{\hat{L}}$ operators justifies the choice of correspondence $\vec{\hat{E}}_r = \gamma\vec{\hat{L}}_r$, since classically, the vectors $\vec{E}$ satisfy the same closure relation (3.3).

3.4.1 The Area Operator

We now show that area is quantised in LQG. Consider the classical discretisation again. The area of a face of a tetrahedron can be calculated with formula:

$$
A^2 = \sum_i E_iE_i = \vec{E}\cdot\vec{E}. \tag{3.37}
$$

In the quantum theory, the area of a face is promoted to an operator $\hat{A}$, which is the simplest gauge invariant operator one can build from $\vec{\hat{E}}$. We would like to find the eigenstates of the area operator:

$$\hat{A}^2\Psi = \hat{\vec{E}} \cdot \hat{\vec{E}}\Psi = \gamma^2 \hat{\vec{L}} \cdot \hat{\vec{L}}\Psi. \tag{3.38}$$

In the derivation (3.35), we have used the result that for elements of Wigner matrices, $\hat{L}_i D^j_{ab}(U) = D^j_{ac}(U) d^j_{cb}(T_i)$. Consider the spin-$\frac{1}{2}$ representation, where $D^{\frac{1}{2}}_{ab}(U) = U_{ab}$. The area operator acting on this matrix gives

$$\begin{aligned} \hat{A}^2 U_{ab} &= \gamma^2 \hat{\vec{L}} \cdot \hat{\vec{L}} U_{ab} \\ &= \gamma^2 \sum_i U_{ac}(T_i)_{cd}(T_i)_{db} \\ &= \gamma^2 \, \frac{3}{4} U_{ab}. \end{aligned} \tag{3.39}$$

The property of Pauli matrices $(\sigma_1)^2 = (\sigma_2)^2 = (\sigma_3)^2 = \mathbb{1}$ was used in the above calculation.

The operators $\hat{L}_i$ satisfy the same commutation algebra as spin in particle mechanics:

$$\left[\hat{L}_i, \hat{L}_j\right] = i\epsilon_i j^k \hat{L}_k. \tag{3.40}$$

Therefore, one should expect the area operator $\hat{A}^2$ to have eigenvalues $\gamma^2 \, j(j+1)$. In general, one can show that the element of a Wigner matrix of spin j is an eigenfunction of the area operator, with the relation

$$\hat{A}^2 D^j_{ab} = \gamma^2 \, j(j+1) D^j_{ab}. \tag{3.41}$$

Thus, we can deduce that the spin network states are eigenstates of the area operator, since such states are decomposed into products of Wigner matrices. We also see that the smallest quantum of area takes discretised values. Reintroducing the physical constants, area eigenvalues are

$$A = \gamma \, {l_p}^2 \sqrt{j(j+1)}, \tag{3.42}$$

where l_p is the Planck length. Furthermore, one may also calculate the area of an arbitrary surface embedded in the manifold:

$$A = \gamma \, {l_p}^2 \sum_r \sqrt{j_r(j_r+1)}, \tag{3.43}$$

summing over all links l_r that "pierce" the surface. This is an important fundamental result of loop quantum gravity: there exists a smallest unit of area, on the scale of ${l_p}^2$.

3.4.2 The Volume Operator

Recall from the classical discretisation that the volume of a tetrahedron is

$$V^2 = \frac{2}{9}\left|\epsilon^{ijk}(E_1)_i(E_2)_j(E_3)_k\right|. \tag{3.44}$$

As it is with the case of area, when the volume equation is promoted to an operator relation, it defines a gauge invariant operator. The volume operator acts on nodes of a spin network state, dual to a tetrahedron in the discretisation. Therefore, its eigenvalue depends on the spins assigned to the four links that join at the node, as well as the virtual spin that labels the 4-valent intertwiner at the node. Rovelli and Vidotto provide a derivation of the eigenstates and eigenvalues in [10], here we quote the result that for a node that joins links with spins j_1, ..., j_4, the eigenstates are superpositions of two spin network states, where the intwrtwiners are labelled with spin k and $k+1$ respectively. The eigenvalues are

$$V = \frac{\sqrt{2}}{3}{l_p}^3\gamma^{\frac{3}{2}}\frac{4}{\sqrt{4k^2-1}}\Delta(j_1+\frac{1}{2}, j_2+\frac{1}{2}, k)\Delta(j_3+\frac{1}{2}, j_4+\frac{1}{2}, k). \tag{3.45}$$

Here, $\Delta(a,b,c)$ is the Heron's formula, which calculates the area of a triangle with side lengths a, b, and c:

$$\Delta(a,b,c) = \frac{1}{4}\sqrt{(a+b+c)(-a+b+c)(a-b+c)(a+b-c)}. \tag{3.46}$$

We again see that, similar to area, there exists a smallest unit of volume, on the order ${l_p}^3$. The area and volume operators form a complete set of commuting observables. Therefore, their eigenvalues completely determine a state in the Hilbert space of LQG. To illustrate the intrinsic "blurriness" of the quantum geometry introduced in LQG, consider a node dual to a tetrahedron. Each 4-valent node in the graph is associated with 5 degrees of freedom: the four areas and the one volume. On the other hand, a tetrahedron classically has 6 degrees of freedom: for example, the length of its 6 edges. This is similar to angular momentum in particle quantum mechanics, where one can only simultaneously diagnalise two operators $\hat{L}^2$ and $\hat{L}_z$. The classical notion of a tetrahedron therefore breaks down at the quantum level, serving only as an analogy for one to better understand the physical quantities in the theory.

4 Dynamics: Constraints, Time Evolution and Transition Amplitudes

The construction of the Hilbert space of loop quantum gravity described in the previous chapter is well established with little ambiguities. For the dynamics of the theory, however, many open problems remain, and there does not exist a consensus on the formulation of the full theory. In general, there are two approaches to generating dynamics in LQG. The first is by solving the canonically quantised version of the Hamiltonian constraint. In the classical theory, constraints generate time evolution from one spacial sub-manifold to succeeding ones, so one may expect the quantum theory to exhibit the same property. The other approach is the "covariant" approach, where path integrals are constructed from spin foams, which are a four dimensional analogue of spin networks. In this chapter, we will examine both approaches, and discuss some proposed models.

4.1 The Momentum Constraint

Up to this point, we have constructed a gauge invariant theory of quantum gravity, solving the Gauss constraint. There are, however, additional constraints remaining, namely the momentum constraint and the Hamiltonian constraint in (2.26). In this section, we address the momentum constraint.

As shown in previous sections, the momentum constraint classically corresponds to the requirement that the theory is invariant under spacial diffeomorphisms. Therefore, the quantum theory satisfies the momentum constraint if it can be shown to be background independent. This condition is in fact automatically satisfied by the theory constructed so far. In the classical discretisation, we considered a graph Γ embedded in a spacial manifold Σ, and defined the holonomies using the embedded path γ_i of each link l_i. This construction is not invariant under diffeomorphism, since the holonomies depend on the background connection field ${A_a}^i$, and transforming the embedding of a link l_i will change the holonomy associated with l_i. However, in the quantum theory, if we interpret the graph Γ as the fundamental structure of spacetime, and the $SU(2)$ group elements U_i as the fundamental variables, the theory no longer depends on the background metric. Rather, the spin network states now define the geometry, through observables such as the area and volume operator.

Figure 4.1: Two graphs that are combinatorially equivalent, but inequivalent under diffeomorphisms.

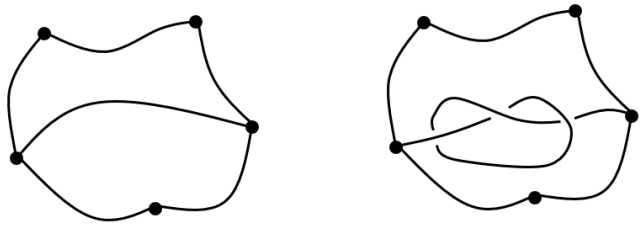

A point of subtlety needs to be addressed: combinatorially equivalent graphs may define inequivalent physical spaces. Figure 4.1 shows two spin networks with equivalent combinatorial structures. However, the graph on the right contains a knot, making it topoligically distinct from the graph on the left; it is impossible to transform the two graphs into each other through continuous deformations. The inequivalent spin networks with different knot structures are known as "knotted spin networks". It is unclear if knotted graphs occur in physical systems, since they cannot be constructed from the dual of a discretisation, and therefore do not have meaningful physical interpretations such as area and volume.

There is a more mathematical construction of solutions of the momentum constraint, following [13] and [14]. We use Ψ_{γ_i} denote states in the Hilbert space constructed by embeddings γ_i of links l_i into the manifold. Consider states to be cylindrical wavefunctionals of the connection: $\Psi_{\gamma_i} = \Psi_{\gamma_i}(U_i[A])$. Consider a diffeomorphism $\chi \in Diff(\Sigma)$, and denote $\mathcal{U}_\chi$ as the operator that transforms a state under the diffeomorphism:

$$\mathcal{U}_\chi \Psi_{\gamma_i}(U_i[A]) = \Psi_{\chi\gamma_i}(U_i[A]). \tag{4.1}$$

From this, we can formally construct a diffeomorphism invariant state:

$$(\,[\Psi_{\gamma_i}]\,| = \sum_{\chi \in Diff(\Sigma)} \langle \Psi_{\gamma_i}| \mathcal{U}_\chi = \sum_{\chi \in Diff(\Sigma)} \langle \Psi_{\chi\gamma_i}|\,. \tag{4.2}$$

The square bracket $[\Psi_{\gamma_i}]$ denotes the equivalence class of states under diffeomorphism, and the rounded bracket emphasises that this is a distributional state that cannot be normalised. It is easy to see that $(\,[\Psi_{\gamma_i}]\,|$ is invariant under diffeomorphisms: $(\,[\Psi_{\gamma_i}]\,|\mathcal{U}_\chi = (\,[\Psi_{\gamma_i}]\,|$. Using this, one can define a diffeomorphism invariant inner product between two states:

$$\left\langle \Psi_{\gamma_i} | \Phi_{\gamma_i'} \right\rangle_{Diff} = \left(\,[\Psi_{\gamma_i}]\,|\Phi_{\gamma_i'}\right\rangle. \tag{4.3}$$

4.2 The Hamiltonian Constraint

Up to this point, the constraint equations have been addressed indirectly: the Gauss constraint was solved by considering gauge transformations, resulting in spin network states; the vector constraints were taken into account if one takes the spin networks to be independent of diffeomorphism. There was no need to explicitly implement the constraint equations as operator relations. The Hamiltonian constraint, however, seems to pose more challenge, since it is related to the reparameterisation of time, which has been neglected in the construction of the theory so far. There is currently no consensus on how the Hamiltonian constraint is to be implemented in loop quantum gravity, although there exist some popular candidate methods. In this section, we review the technique developed by Thiemann [15] to impose the Hamiltonian constraint on states in LQG. Instead of showing the full derivation of the constraint here, the logical outline will be presented, and some key steps will be highlighted.

First, recall the classical form of the Hamiltonian constraint (2.31). We now introduce its smeared form, written as

$$C[g] = \int d^3x\, g\, \frac{\tilde{E}^a_i \tilde{E}^b_j}{\sqrt{det(\tilde{E})}} \left[\epsilon^{ij}{}_k F_{ab}{}^k - 2(1+\gamma^2) K^i{}_{[a} K^j{}_{b]}\right], \tag{4.4}$$

Where $g(x)$ is an arbitrary scalar field. For convenience, we decompose the smeared constraint into two components : $C = C^E - 2(1+\gamma^2)T$, defined as

$$\begin{aligned} C^E[g] &= \int d^3x\, g\, \frac{\tilde{E}^a_i \tilde{E}^b_j}{\sqrt{det(\tilde{E})}} \epsilon^{ij}{}_k F_{ab}{}^k \\ T[g] &= \int d^3x\, g\, \frac{\tilde{E}^a_i \tilde{E}^b_j}{\sqrt{det(\tilde{E})}} K^i{}_{[a} K^j{}_{b]}. \end{aligned} \tag{4.5}$$

The superscript in C^E emphasizes that it is the "Euclidean component" of the constraint. The goal of the following paragraphs is to reformulate (4.4) in terms of the operators of holonomy $\hat{U}$, area $\hat{A}$, and volume $\hat{V}$ defined previously in the quantum theory, and implement it as an operator on physical states, in terms of the condition

$$\hat{C}\, \Psi(U_i) = 0. \tag{4.6}$$

The first trick by Thiemann is the realisation that the variables in the expression of C^E and T can be re-written as Poisson brackets. Introducing quantities

$$\begin{aligned} \bar{K} &= \int d^3x K^i{}_a \tilde{E}^a_i \\ V &= \int d^3x \sqrt{det\tilde{E}}, \end{aligned} \tag{4.7}$$

one finds relations

$$\begin{aligned} K^i{}_a &= \frac{1}{\gamma}\{A^i{}_a, \bar{K}\} \\ \bar{K} &= \frac{1}{\gamma^{\frac{3}{2}}}\{C^E[1], V\} \\ \frac{\tilde{E}^b_i \tilde{E}^c_j}{\sqrt{det(\tilde{E})}} \epsilon^{ijk} \epsilon_{abc} &= \frac{4}{\gamma}\{A^k{}_a, V\}. \end{aligned} \tag{4.8}$$

Using these, the constraints C^E and T can be rewritten as

$$C^E[g] = \int d^3x\, g\, \epsilon^{abc}\delta ij F_{ab}{}^i\{A^j{}_c, V\} = \int d^3x\, g\, \epsilon^{abc} Tr[F_{ab}\{A_c, V\}]$$
$$T[g] = \int d^3x \frac{g}{\gamma^3}\epsilon^{abc}\epsilon_{ijk}\{A^i{}_a, \{C^E[1], V\}\}\{A^j{}_b, \{C^E[1], V\}\}\{A^k{}_c, V\}. \tag{4.9}$$

This formulation allows one to convert the classical constraint into an operator: the Poisson brackets become commutators when the variables become operators.

The next step is to re-express the variables in terms of quantities defined on spin networks. To do this, we notice that the curvature $F_{ab}{}^i$ at some point can be approximated using holonomies of infinitesimal closed paths that start and terminate at that point:

$$U_{\gamma_{ab}} - U^{-1}_{\gamma_{ab}} = AF_{ab}{}^i T_i + \mathcal{O}(A^2), \tag{4.10}$$

γ_{ab} denotes a closed curve oriented in the ab plane, and A is the coordinate area enclosed by γ_{ab}. Similarly, one can find the relation

$$U^{-1}_{\gamma_a}\{U_{\gamma_a}, V\} = l\{A^i{}_a, V\} + \mathcal{O}(l^2), \tag{4.11}$$

γ_a being a path in the direction of coordinate a, with length l. Using these relations, one can write the Hamiltonian constraint in terms of holonomies U and volumes V, which are well defined operators in the quantum theory. In particular, the Euclidean component can be expressed as

$$C^E[g] = \int d^3x\, g\, \frac{1}{Al}\epsilon^{abc} Tr[U_{\gamma_{ab}} - U_{\gamma_{ab}}\{A_c, V\}]. \tag{4.12}$$

The last step is to discretise the integral expressions, so that they can act on spin network states. One can convert integrals into sums over all nodes n_i in a spin network:

$$\int d^3x\, g \;\rightarrow\; \sum_i V_i g_i, \tag{4.13}$$

where V_i is the volume of the tetrahedron dual to node n_i. The volume factor V_i cancels the inverse volume factor $1/Al$ in (4.12), and we can obtain a regularised and well-defined Hamiltonian constraint that acts on states in LQG. The Hamiltonian constraint acts on spin network states by creating and annihilating nodes and links, thereby generating time evolution.

Finally, we discuss the solutions to the quantum Hamiltonian constraint. That is, physical states satisfying the condition $\hat{C}\Psi = 0$. In general, these states take the from of spin networks with "dressed nodes". They are a superposition of spin network states, where the original spin network is modified, including additional links that join the original links around a node.

Figure 4.2: An illustration of dressed nodes that solve the Hamiltonian constraint.

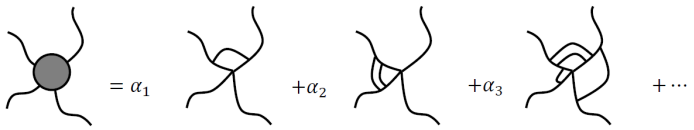

Such dressed nodes are depicted in figure 4.2. On these states, the Hamiltonian constraint will manifest as algebraic relations between coefficients α_n for each graph. The new nodes created in this process are tri-valent. As a result, they do not carry any volume. The information in volume is therefore preserved by the original 4-valent node dual to a tetrahedron. In general, the explicit expressions of states that solve the Hamiltonian constraint is not well known [14]. The definition of the Hamiltonian constraint is not unique, the example presented here being one of the most studied. There are many ambiguities, such as the ordering of operators, that result in mathematically consistent theories. It is not known whether any of the formulations better reproduce classical general relativity in appropriate limits [13].

4.3 Spacetime Discretisation and Spin Foam

Spin foam is an alternative method of defining the dynamics of LQG. It is based on the discretisation of path integrals, which has the advantage of avoiding the complicated form of the Hamiltonian constraint. As a result, full definitions of the dynamics have been completed using the covariant method, allowing for the computation of transition amplitudes. Several different definitions of spin foam theories exist, most of which are conceptually similar, and differ only in small variations. Since an explicit recovery of a classical limit has not been completed, it is difficult to determine which variation is favorable. For this review, we focus on the definition presented in [10].

We consider a section $\mathcal{M}$ of a 4-dimensional spacetime. We assume the boundary $\partial\mathcal{M}$ consists of two disconnected spacelike hypersurfaces: a past boundary denoted Σ_p, and a future boundary Σ_f. The aim is to define quantities on the bulk spacetime $\mathcal{M}$, which allows us to compute transition amplitudes between LQG states defined on Σ_p and Σ_f. The construction here is analogous to that of spin networks. We first discretise $\mathcal{M}$ into 4-simplices, which are 4-dimensional analogues of tetrahedrons. Each 4-simplex is bounded by 5 tetrahedra, which are in turn bounded by triangles. This discretisation is denoted $\Delta_{\mathcal{M}}$. In the 3-dimensional case, a graph was constructed dual to the discretisation. In the 4-dimensional case, we instead construct a "two-complex", which is a graph with additional structures: as in the 3D case, we associate a node n_i to each 4-simplex in the discretisation, and a link l_i to each pair of 4-simplices that share a boundary tetrahedron; furthermore, we associate a face f_i dual to each triangle in the discretisation. These faces are bounded by links in the graph. A two-complex denoted $\Delta^*_{\mathcal{M}}$ is composed of the set of nodes, links and faces.

The two-complex allows us to discretise the generalised tetrad-Palatini action. Recall the form of the action:

$$S[e,\omega] = \int \left(\epsilon_{IJKL} e^K \wedge e^L + \frac{1}{\gamma} e_I \wedge e_J \right) R^{IJ} = \int B_{IJ} R^{IJ}. \tag{4.14}$$

To define the discretised action, we again smear the connection ω and its conjugate momentum B over appropriate regions of the manifold. We choose the connection ω to be an element of the algebra $sl(2,\mathbb{C})$, which is isomorphic to the Lorentz algebra $so(3,1)$, and define a holonomy $U_i \in SL(2,\mathbb{C})$ associated to each link l_i in $\Delta^*_{\mathcal{M}}$:

$$U_i = P e^{\int_{l_i} \omega}. \tag{4.15}$$

The conjugate momentum B is a two-form, so it is natural to integrate it over a 2-dimensional subserface. Thus, we assign an algebra element $B_i \in sl(2,\mathbb{C})$ to each face f_i in the two-complex:

$$B_i = \int_{S_i} B, \tag{4.16}$$

where the range of integration S_i is the triangle in $\Delta_{\mathcal{M}}$ dual to the face f_i. One may notice the problem with defining these smeared variables on the boundaries, where there are incomplete faces and links that do not end at any node. These will be addressed in the next section, for now we focus on the interior of $\Delta_{\mathcal{M}}$.

Using the smeared variables, one can write a discrete action:

$$S = \sum_f Tr \left[B_f \prod_{l \in f} U_l \right], \tag{4.17}$$

where the sum is over all faces in the two-complex, and $l \in f$ refer to the links that bound a face. It can be shown that in the continuous limit, this action approaches (4.14) [10]. The product of holonomies U_l on all links that bound a face f approximates curvature, since it represents the parallel transport along a closed loop around the triangle dual to f. As a result, curvature is only defined in the plane normal to the triangle. It can be defined as a covariant tensor R_{IJ} only when one considers the average of curvatures in a region of the discretised spacetime.

We can now propose a partition function by discretising the path integral:

$$\begin{aligned} \mathcal{Z} = \int \mathcal{D}e \mathcal{D}\omega e^{iS[e,\omega]} &\to \int \prod_f dB_f \prod_i dU_i \, e^{iS[B_f, U_i]} \\ &= A \int \prod_f dB_f \prod_i dU_i \, e^{i \sum_f Tr\left[B_f \prod_{l \in f} U_l\right]}. \end{aligned} \tag{4.18}$$

The factor A represents all irrelevant constants in the equation. The factors B_f can then be integrated out using the definition of the delta function, resulting in (absorbing all 2π factors into A) the expression for the partition function:

$$\mathcal{Z} = A \int \prod_i dU_i \prod_f \delta\left(\prod_{l \in f} U_l\right). \tag{4.19}$$

Effectively, the discretised path integral serves as a regularisation to the continuous theory.

4.4 The Y_γ Map and Transition Amplitudes

The discretisation $\Delta_\mathcal{M}$ naturally defines discretisations of the future and past boundaries into tetrahedrons, denoted Δ_{Σ_p} and Δ_{Σ_f}. One can then construct spin network states on the boundaries following the prescription given in chapter 3. In principle, one can compute the transition amplitude between states on Δ_{Σ_p} and Δ_{Σ_f}, by defining boundary limits in the integration (4.19) based on the boundary wavefunctions, and integrating over all internal links in the two-complex. However, there remain some difficulties. First, states defined on spacial manifolds are wavefunctions of $SU(2)$ group elements, while variables defined on the bulk spacetime are elements of $SL(2,\mathbb{C})$. One needs an appropriate mapping between elements in the two groups. Second, in the disctetisation of a 3-dimensional space, a node is dual to a tetrahedron, and a link is dual to a triangle; for a two-complex on a 4-dimensional spacetime, a node is dual to a 4-simplex, while a link is dual to a tetrahedron. Therefore, more construction is required to produce a precise mapping between boundary wavefunctions and boundary spacetime variables. In this section, we address both problems , and propose a formula for transition amplitudes in LQG, following [10].

There exist different models of LQG resulting from different methods of mapping $SU(2)$ elements into $SL(2,\mathbb{C})$). There we will examine the technique that Rovelli calls the "Y_γ map". We first consider unitary irreducible representations of $SL(2,\mathbb{C})$). Each representation can be labelled with a positive real number p and a half-integer spin k. Noting that $SU(2)$ is a subgroup of $SL(2,\mathbb{C})$), the representation $V^{p,k}$ of $SL(2,\mathbb{C})$) can be written as a tensor sum of $SU(2)$ irreducible representations:

$$V^{p,k} = \bigoplus_{j=k,\, k+1,\, \ldots} \mathcal{H}_j, \tag{4.20}$$

where $\mathcal{H}_j$ is the spin j representation of $SU(2)$, which can be decomposed into basis states $|j,m\rangle$. As a result, a basis state in any unitary representation of $SL(2,\mathbb{C})$ can be labelled with 4 numbers $|p,k;j,m\rangle$.

Now recall from chapter 2 that the momentum 2-form can be decomposed into a "boost" component $K^i = B^{i0}$ and the "rotation" component $L^i = \frac{1}{2}\epsilon^i_{jk}B^{jk}$, with the linear simplicity constraint $K^i = \gamma L^i$. This constraint holds also for the smeared variable $B_f = \int_{S_f} B$. Since B_f is an element of $sl(2,\mathbb{C})$, we can consider its action as generators of $SL(2,\mathbb{C})$ on the states

$|p,k;j,m\rangle$. Then the spin j is the eigenvalue of $\vec{L}^2$, and m can be set as the eigenvalue of L^z. There are two Casimir invariants in $sl(2,\mathbb{C})$:

$$\begin{aligned} C_1 &= \frac{1}{2}B_{IJ}B^{IJ} = \vec{K}^2 - \vec{L}^2 \\ C_2 &= \frac{1}{8}\epsilon_{IJKL}B^{IJ}B^{KL} = \vec{K}\cdot\vec{L}. \end{aligned} \tag{4.21}$$

One can show that, acting on the basis states, the two Casimirs give the relations

$$\begin{aligned} C_1\,|p,k;j,m\rangle &= (p^2 - k^2 + 1)\,|p,k;j,m\rangle \\ C_2\,|p,k;j,m\rangle &= pk\,|p,k;j,m\rangle\,. \end{aligned} \tag{4.22}$$

Thus, imposing the linear simplicity constraint on the basis states with $K^i\,|p,k;j,m\rangle = \gamma L^i\,|p,k;j,m\rangle$, we find that they must satisfy the relation

$$p = \gamma k,\ k = j. \tag{4.23}$$

This allows us to relate states in $SU(2)$ representations into states in $SL(2,\mathbb{C})$ representations using the Y_γ map:

$$\begin{aligned} Y_\gamma : \mathcal{H}_j &\to V^{(\gamma j, j)} \\ |j,m\rangle &\to |\gamma j, j; j, m\rangle\,. \end{aligned} \tag{4.24}$$

This is the map that we will use to convert $SU(2)$ variables on the spin networks into $SL(2,\mathbb{C})$ variables on the boundary of the two-complex of spacetime.

For the next step, Rovelli introduces an alternative construction of the spin foam path integral, which allows one to map spin networks onto the boundary of the bulk discretisation. Instead of assigning one holonomy U_l to each link l, we assign two $SL(2,\mathbb{C})$ elements. One may interpret this as identifying a mid-point of the link, and associating a holonomy to each segment. These elements are denoted g_{lv}, labelled by the link and vertex adjacent to the segment of the link. The path integral (4.19) is rewritten using twice as many variables:

$$\mathcal{Z} = A\int \prod_{lv} dg_{lv} \prod_f \delta\left(\prod_{g\in f} g\right). \tag{4.25}$$

The factor A again absorbs extra constants resulting from integrations. Next, we assign an $SL(2,\mathbb{C})$ element to each pair of links that join at a node, and bound the same face. These elements are labelled h_{vf}, identified by the vertex and face they are adjacent to. The path integral (4.25) can then be rewritten as

Figure 4.3: The assignment of group elements for internal and boundary faces. The dotted lines represent links, and the solid lines represent the assignment of h. Figure sourced from [10].

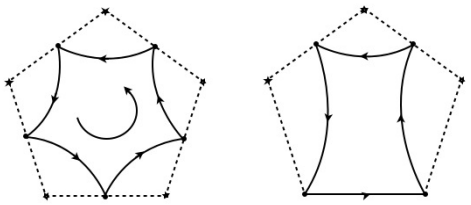

$$\mathcal{Z} = A \int \prod_{vf} dh_{vf} \prod_{f} \delta \left(\prod_{h \in f} h \right) \prod_{v} A_v, \tag{4.26}$$

where A_v is the "vertex amplitude":

$$A_v = \sum dg' \prod_{f} \delta \left(g' g h_{vf} \right), \tag{4.27}$$

g' and g are the two $SL(2, \mathbb{C})$ elements adjacent to h_{vf}.

To compute the transition amplitude, we consider the combined graph of the bulk and boundary discretisation. This graph will contain bulk links, dual to internal tetrahedra, and boundary links, dual to triangles. The product $(\prod_{h \in f} h)$ is defined as illustrated by figure 4.3. For an internal face, bounded only by internal links, the group elements h are assigned according to the left figure. For a face bounded by a boundary link, the group elements are assigned according to the right figure, where the bottom link is the boundary link. Applications of this definition of the transition amplitude has produced successful results, some of which will be discussed in the following chapters.

5 Application: Black Holes

In section 3, we have studied the kinematics of loop quantum gravity, defining the Hilbert space and some observables. In section 4, we discussed some proposed methods of completing the full theory, where transition amplitudes may be calculated. In the following sections, we will examine some physical applications of the theory. From a successful theory of quantum gravity, one should be able to generate classical general relativity in appropriate limits. Unfortunately, the task of explicitly recovering the classical theory from LQG is still incomplete. On the other hand, much progress has been made in applying loop quantum gravity in situations where the classical theory is expected to fail, and quantum effects become significant: namely, spacetime singularities occurring in black holes and the cosmology of the early universe. In this chapter, we shall examine some results in applying LQG to black holes: a calculation of the black hole entropy, and a prediction of what happens at end of a black hole's life time.

5.1 Black Hole Thermodynamics

Bekenstein [16] [17] and Hawking [18] showed that black holes exhibit thermodynamic properties. One can define the three laws of thermodynamics on a black hole, whose entropy is proportional to the area of its event horizon, given by the Bekenstein-Hawking entropy [19]:

$$S = \frac{k_b c^3}{4\hbar G} A. \tag{5.1}$$

This formula can be derived through considerations of quantum fields on a classical curved background. Since it is not derived from a fundamental theory of quantum gravity where both matter and spacetime are quantised, there exist different interpretations of the statistical origin of the entropy. Loop quantum gravity provides a solution to this problem. As a foundational theory of spacetime, it has been shown that LQG predicts the existence of black hole entropy. In this section, we study a derivation of the entropy of a Schwarzschild black hole using LQG spin networks, presented in [20] and [21].

Some useful results shall be quoted here without proof. The first is the energy of a Schwarzschild black hole, measured by a stationary observer at a distance d from the horizon. In order for the observer to remain stationary within the gravitational field, they must maintain an acceleration $a = 1/d$. This observer measures the black hole to have energy

$$E = \frac{Aa}{8\pi G}, \tag{5.2}$$

A being the area of the horizon. Second, the Unruh temperature, measured by an accelerating observer in vacuum [22]:

$$T = \frac{\hbar a}{2\pi k_B}. \tag{5.3}$$

Consider now a spin network embedded in a Schwarzschild spacetime. The event horizon is pierced by a number of links. The spins associated with these links then determine the area of the horizon. A patch of the horizon pierced by a single link may have area eigenvalues

$$A_j = \gamma (l_p)^2 \sqrt{j(j+1)}. \tag{5.4}$$

We may then use (5.2) to find the energy associated with a patch of the horizon to be

$$E_j = a\gamma \sqrt{j(j+1)}. \tag{5.5}$$

Since there is a degeneracy of $2j+1$ for each area eigenvalue, the probability distribution, at temperature T, for the patch of horizon to have area A_j is

$$p_j(T) = \frac{1}{Z(T)}(2j+1)e^{-\frac{E_j}{k_B T}}, \tag{5.6}$$

where $Z(T)$ is the partition function. If one sets T as the Unruh temperature from (5.3), one finds the probability distribution

$$p(T,j) = \frac{1}{Z(T)}(2j+1)e^{-2\pi\gamma\sqrt{j(j+1)}}. \tag{5.7}$$

Using the Gibbs entropy

$$S = -\sum_j p_j log(p_j), \tag{5.8}$$

one finds the entropy associated with the patch of the horizon to be

$$S = \frac{A}{4G} + log(Z). \tag{5.9}$$

The first term is the Bekenstein-Hawking entropy. The second term vanishes if the equation

$$1 = Z = \sum_j (2j+1)e^{-2\pi\gamma\sqrt{j(j+1)}} \tag{5.10}$$

is satisfied. The solution for this can be found numerically to be $\gamma = \gamma_0 \approx 0.274$. This is a critical parameter of LQG. If γ takes this value, then one successfully derives the Bekenstein-Hawking entropy. An alternative calculation of the black hole entropy, presented in [23], considers the entanglement entropy from $SL(2,\mathbb{C})$ coherent states, which exactly recovers the Bekenstein-Hawking entropy, independent of the value of γ. The calculation of black hole entropy from first principles in loop quantum gravity provides a strong argument for its validity as a fundamental theory of quantum gravity.

5.2 Black Hole to White Hole Transition

Hawking [24] showed that black holes emit thermal radiation, and as a result, a black hole loses its mass over its lifetime, and the area of its event horizon gradually reduces. The temperature of the radiation increases as the mass of a black hole decreases, with formula

$$T = \frac{\hbar c^3}{8\pi G k_B M} \tag{5.11}$$

for a Schwarzchild black hole. A solar mass black hole is expected to have a life time on the order of 10^{67} years before completely evaporating [25]. An alternative estimate [26] suggests that the life time of a black hole is roughly proportional to the square of its initial mass. A lunar mass black hole, as a result, may have a life time on the same order as the age of the universe, meaning end stages of primordial black holes may, at least in principle, be observable today. Although lacking in observational evidence, the gradual evaporation of a black hole has become a widely accepted prediction in theoretical physics. What is currently unknown, however, is what occurs near the end of the life time of a black hole. As the mass of the black hole reduces, the intensity of Hawking radiation increases, and area of its event horizon approaches the Planck scale. It is widely conjectured that, at this stage, quantum gravitational effects become significant, and it is no longer accurate to model the phenomenon as quantum perturbations over a classical spacetime. The behaviour of the black hole, in this case, deviates from Hawking's predictions. One of the proposed scenarios is that, toward the end of a black hole's evaporation, it transitions into a white hole through quantum tunnelling. White holes are not known to emerge from any classical process. However, it may be possible that they are the product of some quantum effect. This result has been discussed using generic quantum gravity arguments [27]. However, an explicit calculation of the black hole to white hole transition amplitude has been done using LQG [28] [29]. Here, we will summarise [30] and [26], which provide a simplified calculation that gives an estimation of the transition amplitude.

This calculation makes several assumptions that makes the exact scenario likely unphysical, but the hope is that a real black hole may be constructed through modifications that do not drastically change the order of magnitude of the restult, so it is still valid as a rough estimation. First, the back hole is assumed to form from the collapse of a spherical shell of matter. Second, Hawking radiation is neglected. While the effect of black hole radiation is small for any given time, it is unclear whether quantum effects from the radiation build up thrughout the lifetime of the black hole. The core assumption is that, as the spherical shell collapses to the Schwarzschild radius, a black hole will form. As the shell then approaches Planck size, it will undergo a quantum bounce, and begin to expand outward. From the view of an outside observer, they will perceive the collapse of the shell to slow down and red-shift as its radius approaches the Schwarzschild radius. After some possibly very long amount of time, the black hole will transition into a white hole, and the observer will see the shell re-emerge from within the Schwarzschild radius. In such a picture, there is no event horizon: matter that fall into the black hole will eventually be emitted out of the white hole. What we perceive as a black hole is instead enclosed by an "apparent horizon" that does not entrap infalling matter for an infinite time. The possible absence of an event horizon in such

Figure 5.1: The Carter-Penrose diagram for the black hole to white hole transition form the collapse of a massive shell. Figure sourced from [30].

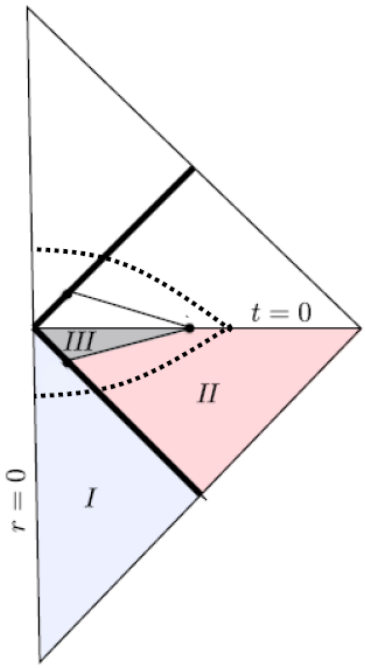

scenarios provides potential solution to the black hole information paradox, and has lead to Hawking's statement that "there are no black holes" [31].

Apart from regions of high curvature around the black and white hole singularity, spacetime is well approximated by classical general relativity. Neglecting small regions where quantum effects are significant, one may still construct a classical geometry that describes the spacetime where this transition takes place. The Carter-Penrose diagram for this spacetime can be constructed from sections of the diagram for a maximally extended Schwarzschild spacetime. In figure 5.1, the bold black lines depict the collapse and rebounce of the massive shell. Region I inside the shell is flat and isomorphic to a Minkowski spacetime, while region II outside the shell has the geometry of a Schwarzschild spacetime. Region III is where quantum effects are expected to take place, and a diagram cannot be drawn. Figure 5.2 demonstrates the construction of this spacetime from patches of the maximally extended Schwarzschild spacetime. This is known as a Haggard-Rovelli spacetime [32], the behaviour of which is symmetric under time reversal: that is, the evolution of the white hole and the expanding shell is identical to the reversed motion of the black hole and the collapsing shell. This is obviously unphysical, since additional effects such as Hawking radiation have been ignored. Nontheless, this simplified model is a good starting point to investigate the decay of a black hole.

Transition amplitudes can be calculated following the procedures defined in the previous sections: we first discretise a bulk section of spacetime, then define spin network states

Figure 5.2: Construction of the bounce spacetime from the maximally extended Schwarzschild spacetime. Figure sourced from [30].

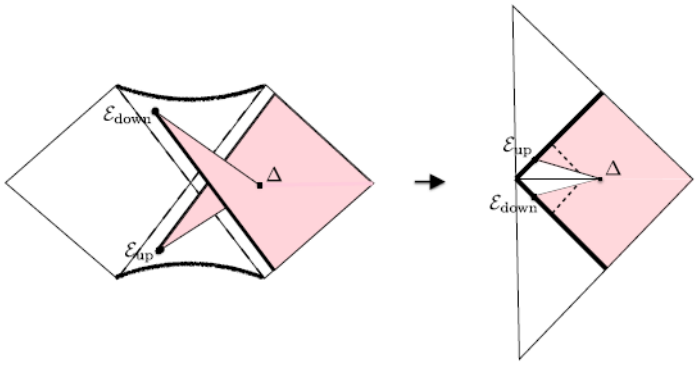

on the boundary of the discretisation. The boundary can be chosen as the dotted lines in figure 5.1, which has the topology of two 3-balls joined at their boundaries. An appropriate discretisation can then be selected, for example, [26] chose to discretise each 3-ball into four tetrahedra. The result shows that the transition amplitude is a function of the initial mass of the collapsing shell, and the time elapsed after the collapse: $W(m, T)$. The average life time of the black hole can then be estimated numerically, which appears to scale with the square of the mass: $\tau \sim m^2$. Since this result is estimated from a drastically simplified model, one should not place full trust on its validity. An alternative construction, demonstrated in [32], results in an estimate of the life time:

$$\tau = me^{\frac{m^2\Xi}{\hbar G}}, \tag{5.12}$$

for a constant Ξ. In conclusion, although there have been numerous attempts to predict the final stage of the life time of a black hole, no consensus has been reached. Nonetheless, an astrophysical observation of a white hole may be considered strong evidence for the validity of LQG.

6 Application: Cosmology

Around the turn of the century, Bojowald [33], Ashtekar [34] and others begin applying techniques developed in loop quantum gravity to the construction of cosmological models. This lead to the establishment of loop quantum cosmology, which describes the quantum behaviour of highly symmetric spacetimes. LQC has produced promising results, such as the resolution of the big bang singularity. However, due to many of the assumptions made in the construction, it is unknown if the predictions are valid in the full theory. In this section, we will discuss some of the results obtained from LQC.

6.1 Classical Cosmology

We first discuss classical cosmology. For simplicity, consider a universe without spacial curvature. Assuming homogeneity and isotropy, this universe is described by the $k = 0$ FLRW metric:

$$ds^2 = -dt^2 + a^2(dx^2 + dy^2 + dz^2). \tag{6.1}$$

The spacial component of a flat universe can either be compact, with the topology of a torus T^3, or non-compact, with the topology of $\mathbb{R}^3$. The two cases need to be treated slightly differently: for the compact case, the scale factor a can be set to measure the volume of the entire universe; for the non-compact case, one may introduce a cubical fiducial cell $\mathcal{C}$. The scale factor then measures the volume of this cell. Results obtained from final theory should be independent from the choice of this cell, with appropriate limits when $\mathcal{C}$ approaches $\mathbb{R}^3$.

To enrich the dynamics of this universe, matter is coupled to the gravitational action. In the literature, this matter often takes the form of a scalar field ϕ, whose field strength, due to homogeneity, is assumed to be uniform in space. The full action therefore consists of a gravitation component, and a matter component:

$$S = S_g + S_m. \tag{6.2}$$

The cosmological constant Λ has been neglected up to this point. Here, we introduce it into the theory, so the gravitation part of the action is

$$S_g = \frac{1}{16\pi G} \int d^4x \sqrt{-g}(R - 2\Lambda). \tag{6.3}$$

We now describe this universe in terms of the ashtekar variables. In a homogeneous and isotropic universe, the connection and the triad can be chosen to take simple forms:

$$\begin{aligned} A_a^i &= \tilde{c}\delta_a^i, \\ E_i^a &= \tilde{p}\delta_i^a, \end{aligned} \tag{6.4}$$

where $\tilde{c} = \gamma\dot{a}$ and $\tilde{p} = a^2$. These variables satisfy the Poisson bracket

$$\{\tilde{c}, \tilde{p}\} = \frac{8\pi G\gamma}{3V_0}. \tag{6.5}$$

For a compact space, V_0 refers to the comoving volume of the universe. For a non-compact universe, V_0 is the comoving volume of the fiducial cell $\mathcal{C}$. It is possible to fix $V_0 = 1$ by re-scaling the dynamical variables: redefining $c = {V_0}^{1/3}\tilde{c}$ and $p = {V_0}^{2/3}\tilde{p}$, one obtains the Poisson bracket $\{c, p\} = 8\pi G\gamma/3$. In the normalisation where $V_0 = 1$, the scale factor a^3 describes the physical volume of the universe [10]. Since a matter field is coupled to this universe, the Hamiltonian constraint consists of a gravitational part and a matter part: $C = C_g + C_m$. The gravitational component can be expressed with the variables c and p, which reads

$$C_g = (\frac{cp}{\gamma})^2 - \frac{\Lambda}{3}p^3. \tag{6.6}$$

Imposing the Hamiltonian constraint $C = C_g + C_m = 0$, one obtains the Friedmann equation

$$(\frac{\dot{a}}{a})^2 = \frac{\Lambda}{3} + \frac{8}{3}\pi G\rho, \tag{6.7}$$

where the matter density ρ is defined as

$$\rho = a^3\frac{\delta S_m}{\delta N}. \tag{6.8}$$

It is common to introduce an alternative set of variables:

$$\begin{aligned} b &= \frac{c}{|p|^{1/2}}, \\ v &= sgn(p)\frac{|p|^{3/2}}{2\pi G}. \end{aligned} \tag{6.9}$$

Notably, v is proportional to a^3 and therefore is a volume variable. These variables satisfy the Poisson bracket $\{b, v\} = 2\gamma$. For a universe only inhabited by a scalar field, the sign on p is associated with the orientation of the triad and does not affect the dynamics: a sign inversion can be regarded as a remarameterisation symmetry. However, if the spacetime is coupled to a spinor field, the sign on p will affect the equations of motion. For this universe, the classical solutions to the equations of motion can be expressed relationally, using v and the scalar field strength ϕ:

$$\phi = \pm\frac{1}{\sqrt{2\pi G}}ln(\frac{v}{v_0}) + \phi_0, \tag{6.10}$$

where v_0 and ϕ_0 are constants that can be fixed by boundary constraints. The scalar field strength ϕ can be regarded as an internal time, with respect to which the evolution of the universe is measured. The plus and minus signs correspond to two distinct solutions: an expanding universe that begins at a big bang, and a contracting universe that end at a big crunch. In the following section, we shall see how the quantum theory may suggest that, as the matter density approaches the Planck scale, the evolution of the universe deviates from the classical trajectory, and the contracting universe transitions into the expanding universe, resulting in a big bounce.

6.2 Loop Quantisation of Cosmology and the Big Bounce

This section follows the discussions in [35] and [36]. For this highly symmetric universe with reduced degrees of freedom, the quantisation follows a similar procedure as the full theory of LQG: we smear the connection over a path to obtain a holonomy. We choose the path to be a straight line with comoving length μ, parallel to the k^{th} direction. The holonomy of the isotropic connection has a simple form:

$$U_k = e^{\mu c T_k} = cos(\frac{\mu c}{2})\mathbb{1} + 2sin(\frac{\mu c}{2})T_k. \tag{6.11}$$

It is thus sufficient to describe the holonomy with a function $N_\mu = e^{i\mu c/2}$. Since the triad is constant in a homogeneous universe, there is no need to smear it over some area, and one can simply use p as the variable for the conjugate momentum. These variables satisfy the Poisson bracket

$$\{N_\mu, p\} = \frac{8\pi i\gamma G}{3}\frac{\mu}{2}N_\mu. \tag{6.12}$$

The quantum theory is constructed by promoting these variables into operators $\hat{N}_\mu$, $\hat{p}$. The wavefunctions in this system are square-integrable functions of the length parameter and the scalar feield strength $\Psi(\mu, \phi)$, with the action of the operators defined as

$$\begin{aligned} \hat{p}\Psi(\mu,\phi) &= \frac{8\pi\gamma l_p^2}{6}\mu\Psi(\mu,\phi), \\ N_\chi\Psi(\mu,\phi) &= \Psi(\mu+\chi,\phi). \end{aligned} \tag{6.13}$$

For the dynamics of this quantum system, we construct the Hamiltonian constraint in a similar fashion as discussed in chapter 4: the curvature tensor ${F_{ab}}^i$ is approximated with holonomies of small loops in the ab plane, and integrals are replaced with finite sums, giving rise to a discretised constraint. The resulting Hamiltonian constraint in loop quantum consmology can be expressed as the following equation:

$$\frac{\partial^2}{\partial\phi^2}\Psi(\mu,\phi) = -\Theta\Psi(\mu,\phi), \tag{6.14}$$

Figure 6.1: The evolution of a spacially flat FLRW universe, as predicted by classical cosmology versus loop quantum cosmology. Figure sourced from [36].

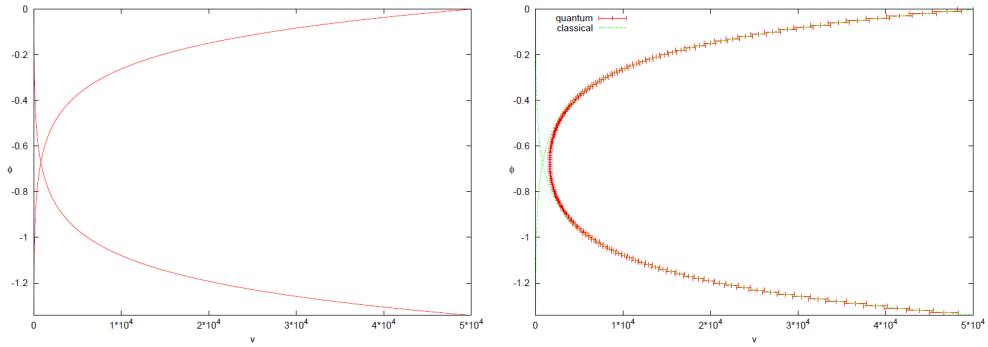

where Θ is the discretised analogy of a differential operator, known as a "difference operator", whose action is defined as

$$\Theta\Psi(\mu,\phi) = -\frac{3\pi G}{4\lambda^2}\mu\left[(\mu+2\lambda)\Psi(\mu+2\lambda,\phi) - 2\mu\Psi(\mu,\phi) + (\mu-2\lambda)\Psi(\mu-4\lambda,\phi)\right], \quad (6.15)$$

where $\lambda = (4\sqrt{3}\pi)^{\frac{1}{2}} l_p$ is a constant, which arises from the consideration that, due to the existence of a minimum area in LQG, when approximating curvature using holonomies, the area of the loop cannot be continuously brought to zero. The Hamiltonian constraint (6.14) describes the evolution of a quantum state with respect to the field strength ϕ. Similar to the classical equation (6.10), the description of the dynamics does not involve an explicit time coordinate.

Figure 6.1 compares the classical and quantum evolution of the universe. On the left, equation (6.10) is plotted, showing the evolution of the volume parameter v with respect to the field strength ϕ. As explained before, there are two solutions, one expanding and one contracting. The graph on the right plots the expectation values of operator $\hat{v}$ on quantum states that solve the Hamiltonian constraint. These states are chosen by starting with a minimal uncertainty state peaked at some large value of v, then evolving it with (6.14). It is easy to see that, at large values of v, the quantum trajectory is well approximated by the classical solution. However, as the universe shrinks and v approaches unity, the quantum universe transitions from the contracting trajectory to the expanding trajectory, resulting in a bouncing universe. In addition, it has been shown [37] [38] that loop quantum cosmology produces an effective Friedmann equation, which modifies the classical equation with an additional term:

$$\left(\frac{\dot{a}}{a}\right)^2 = \frac{8\pi G}{3}\rho(1-\frac{\rho}{\rho_0}) \quad (6.16)$$

where $\rho_0 \approx 0.41\rho_p$ is predicted to be the maximum matter density on the order of the Planck density. This modification generates an effective repulsive force when matter density approaches ρ_0, giving rise to a big bounce. The prediction of a bouncing universe from LQC

Figure 6.2: On the left: the dipole graph, representing two tetrahedra joined together. On the right: the graph representing discretisation of S^3 with five tetrahedra.

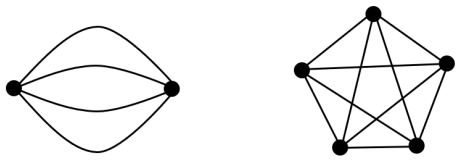

provides argument in favor of LQG, as it is expected to remove singularities that plague classical general relativity. However, since LQC is a highly simplified theory, it is unknown if the full theory of LQG can reproduce the same predictions. Solutions of loop quantum cosmology without a bounce have also been constructed, further casting doubt over the big bounce picture [39] [40].

A more recent development has been attempts to apply covariant loop quantum gravity to cosmological settings, in what is known as "spinfoam cosmology" [41] [42]. As opposed to a model with reduced degrees of freedom which gives rise to LQC, spinfoam cosmology begins with the full theory of LQG. Thus, it is expected to produce stronger predictions that do not depend on the truncation of the theory. Compared to LQC, however, there has been limited development in spinfoam cosmology. The idea is to construct homogeneous states from the quantum theory. A spacial manifold with spherical topology S^3 can be discretised into symmetric graphs. The simplest of which is known as a dipole graph, which is dual to two tetrahedra, with their faces joined to each other. A slightly more complex discretisation uses 5 tetrahedra, as illustrated in figure 6.2. One then defines coherent states on such graphs. These are states that satisfy the minimal uncertainty principle, and in the limit where the spins j become large, are well approximated by classical geometry, analogous to wave packets in particle quantum mechanics. They have been demonstrated to solve the Hamiltonian constraint in the limit where the length scale is large, through transition amplitude calculations.

7 Miscellaneous Aspects and Final Remarks

Due to the limited time span available to complete this review, many aspects of the theory could not be explored in depth. Here, some additional topics shall be briefly discussed.

Cosmological constant and IR regularisation

The discreteness of the geometry of LQG provides a length scale cutoff, and removes UV divergences in quantum gravity. There are however additional divergent quantities remaining in the transition amplitudes. Consider a 4-simplex in the spacetime discretisation. By placing a point inside and connecting it to the vertices, the 4-simplex can be divided into 5 smaller 4-simplices. From this modification, one would obtain the same transition amplitude, except with an additional delta function in the expression, which diverges. It has been shown [43] that such infinities can be removed in a theory with a positive cosmological constant. This result is in agreement with current observations [44].

Coupling with matter

The difficulty of coupling LQG to matter has long been a criticism to the theory. A method has been proposed, however, that allows the quantum geometry of spin foam to be coupled with Fermions [45], by constructing a modified Fermion action. Consider a chiral spinor field ψ. The projection of the Dirac action onto one of its helicity states gives

$$S = i \int d^4x \, \bar{\psi} \sigma^\mu \partial_\mu \psi, \tag{7.1}$$

where $\sigma^\mu = (\mathbb{1}, \sigma^i)$ are the Pauli matrices. This action can be discretised by assigning a spinor field to each link l in the spin foam: $\psi(x) \to \psi_l$. The resulting action reads

$$S = i \sum_{l,l'} \bar{\psi}_{l'} V_l \sigma_l \psi_l, \tag{7.2}$$

where V_l is the volume of the tetrahedron dual to l, σ_l is the projection of the vector-matrix σ^μ in the direction of the link l, and the indices l, l' sum over pairs of links that share a node. This action is defined on the same physical space as spin foam variables, allowing interactions between them. Little is known still on explicitly coupling the standard model to loop quantum gravity.

Propagation of light

Some have proposed that LQG may produce observable effects on high energy gamma ray bursts [4]. Based on dimensional estimations, the quantum geometry may affect the speed of light propagation on the order l_p/λ, where l_p is the Planck length and λ is the wavelength of light. Although the order of magnitude of this effect is very small, it may cause measurable

differences in the arrival time of gamma rays from bursts up to 10^{10} light years away. However, this effect is predicted based on rough estimations, and its validity cannot be verified.

Although loop quantum gravity has produced many elegant results, much work remains in refining it into a mathematically consistent and physically realistic theory with testable predictions. It remains to be seen whether it will rise above the rest to become the definitive theory of quantum gravity.

References

[1] B. S. DeWitt, "Quantum Theory of Gravity. 1. The Canonical Theory," *Phys. Rev.*, vol. 160, L.-Z. Fang and R. Ruffini, Eds., pp. 1113–1148, 1967. DOI: 10.1103/PhysRev.160.1113.

[2] A. Ashtekar, "New Variables for Classical and Quantum Gravity," *Phys. Rev. Lett.*, vol. 57, pp. 2244–2247, 1986. DOI: 10.1103/PhysRevLett.57.2244.

[3] T. Thiemann, "Modern canonical quantum general relativity," 2001. arXiv: gr-qc/0110034.

[4] R. Gambini, *A first course in loop quantum gravity*, eng. Oxford: Oxford University Press, 2011, ISBN: 0199590753.

[5] A. Ashtekar, "Ashtekar variables," *Scholarpedia*, vol. 10, no. 6, p. 32 900, 2015, revision #186565. DOI: 10.4249/scholarpedia.32900.

[6] R. Gambini, *Loops, knots, gauge theories, and quantum gravity*, eng, ser. Cambridge monographs on mathematical physics. Cambridge ; Cambridge University Press, 1996, ISBN: 0-511-52443-9.

[7] R. Giles, "Reconstruction of gauge potentials from wilson loops," *Phys. Rev. D*, vol. 24, pp. 2160–2168, 8 Oct. 1981. DOI: 10.1103/PhysRevD.24.2160. [Online]. Available: https://link.aps.org/doi/10.1103/PhysRevD.24.2160.

[8] T. Regge, "GENERAL RELATIVITY WITHOUT COORDINATES," *Nuovo Cim.*, vol. 19, pp. 558–571, 1961. DOI: 10.1007/BF02733251.

[9] R. R. Cuzinatto, C. A. M. de Melo, and C. N. de Souza, *Introduction to regge calculus for gravitation*, 2019. arXiv: 1904.01966 [gr-qc].

[10] C. Rovelli and F. Vidotto, *Covariant Loop Quantum Gravity: An Elementary Introduction to Quantum Gravity and Spinfoam Theory*. Cambridge University Press, 2014. DOI: 10.1017/CBO9781107706910.

[11] C. Rovelli, *Introduction to loop quantum gravity - carlo rovelli*, Quantum Gravity at CPT Marseille, 2018. [Online]. Available: https://www.youtube.com/playlist?list=PLwLvxaPjGHxR6zr421tXXlaDGbq8S36Un.

[12] J. S. Engle, "Spin foams," *Springer Handbook of Spacetime*, pp. 783–807, 2014. DOI: 10.1007/978-3-642-41992-8_38. [Online]. Available: http://dx.doi.org/10.1007/978-3-642-41992-8_38.

[13] A. Perez, "Introduction to loop quantum gravity and spin foams," in *2nd International Conference on Fundamental Interactions*, Sep. 2004. arXiv: gr-qc/0409061.

[14] P. Doná and S. Speziale, *Introductory lectures to loop quantum gravity*, 2010. arXiv: 1007.0402 [gr-qc].

[15] T. Thiemann, "Anomaly-free formulation of non-perturbative, four-dimensional lorentzian quantum gravity," *Physics Letters B*, vol. 380, no. 3-4, pp. 257–264, Jul. 1996, ISSN: 0370-2693. DOI: 10.1016/0370-2693(96)00532-1. [Online]. Available: http://dx.doi.org/10.1016/0370-2693(96)00532-1.

[16] J. D. Bekenstein, "Black holes and the second law," *Lett. Nuovo Cim.*, vol. 4, pp. 737–740, 1972. DOI: 10.1007/BF02757029.

[17] J. D. Bekenstein, "Black holes and entropy," *Phys. Rev. D*, vol. 7, pp. 2333–2346, 1973. DOI: 10.1103/PhysRevD.7.2333.

[18] S. W. Hawking, "Black Holes and Thermodynamics," *Phys. Rev. D*, vol. 13, pp. 191–197, 1976. DOI: 10.1103/PhysRevD.13.191.

[19] J. D. Bekenstein, "Bekenstein-Hawking entropy," *Scholarpedia*, vol. 3, no. 10, p. 7375, 2008, revision #182595. DOI: 10.4249/scholarpedia.7375.

[20] C. Rovelli, "Black hole entropy from loop quantum gravity," *Physical Review Letters*, vol. 77, no. 16, pp. 3288–3291, Oct. 1996, ISSN: 1079-7114. DOI: 10.1103/physrevlett.77.3288. [Online]. Available: http://dx.doi.org/10.1103/PhysRevLett.77.3288.

[21] A. Ashtekar, J. Baez, A. Corichi, and K. Krasnov, "Quantum geometry and black hole entropy," *Physical Review Letters*, vol. 80, no. 5, pp. 904–907, Feb. 1998, ISSN: 1079-7114. DOI: 10.1103/physrevlett.80.904. [Online]. Available: http://dx.doi.org/10.1103/PhysRevLett.80.904.

[22] W. G. Unruh, "Notes on black hole evaporation," *Phys. Rev. D*, vol. 14, p. 870, 1976. DOI: 10.1103/PhysRevD.14.870.

[23] E. Bianchi, *Entropy of non-extremal black holes from loop gravity*, 2012. arXiv: 1204.5122 [gr-qc].

[24] S. W. Hawking, "Particle Creation by Black Holes," *Commun. Math. Phys.*, vol. 43, G. W. Gibbons and S. W. Hawking, Eds., pp. 199–220, 1975, [Erratum: Commun.Math.Phys. 46, 206 (1976)]. DOI: 10.1007/BF02345020.

[25] R. Parentani and P. Spindel, "Hawking radiation," *Scholarpedia*, vol. 6, no. 12, p. 6958, 2011, revision #135540. DOI: 10.4249/scholarpedia.6958.

[26] M. Christodoulou, C. Rovelli, S. Speziale, and I. Vilensky, "Planck star tunneling time: An astrophysically relevant observable from background-free quantum gravity," *Physical Review D*, vol. 94, no. 8, Oct. 2016, ISSN: 2470-0029. DOI: 10.1103/physrevd.94.084035. [Online]. Available: http://dx.doi.org/10.1103/PhysRevD.94.084035.

[27] E. Bianchi, M. Christodoulou, F. D'Ambrosio, H. M. Haggard, and C. Rovelli, "White holes as remnants: A surprising scenario for the end of a black hole," *Classical and Quantum Gravity*, vol. 35, no. 22, p. 225 003, Oct. 2018, ISSN: 1361-6382. DOI: 10.

1088/1361-6382/aae550. [Online]. Available: http://dx.doi.org/10.1088/1361-6382/aae550.

[28] F. D'Ambrosio, M. Christodoulou, P. Martin-Dussaud, C. Rovelli, and F. Soltani, "End of a black hole's evaporation," *Physical Review D*, vol. 103, no. 10, May 2021, ISSN: 2470-0029. DOI: 10.1103/physrevd.103.106014. [Online]. Available: http://dx.doi.org/10.1103/PhysRevD.103.106014.

[29] F. Soltani, C. Rovelli, and P. Martin-Dussaud, *The end of a black hole's evaporation – part ii*, 2021. arXiv: 2105.06876 [gr-qc].

[30] H. M. Haggard and C. Rovelli, "Quantum-gravity effects outside the horizon spark black to white hole tunneling," *Physical Review D*, vol. 92, no. 10, Nov. 2015, ISSN: 1550-2368. DOI: 10.1103/physrevd.92.104020. [Online]. Available: http://dx.doi.org/10.1103/PhysRevD.92.104020.

[31] Z. Merali, "Stephen hawking: 'there are no black holes'," *Nature*, 2014. [Online]. Available: https://doi.org/10.1038/nature.2014.14583.

[32] M. Christodoulou and F. D'Ambrosio, *Characteristic time scales for the geometry transition of a black hole to a white hole from spinfoams*, 2018. arXiv: 1801.03027 [gr-qc].

[33] M. Bojowald, "Loop quantum cosmology. I. Kinematics," *Class. Quant. Grav.*, vol. 17, pp. 1489–1508, 2000. DOI: 10.1088/0264-9381/17/6/312. arXiv: gr-qc/9910103.

[34] A. Ashtekar, M. Bojowald, and J. Lewandowski, "Mathematical structure of loop quantum cosmology," *Adv. Theor. Math. Phys.*, vol. 7, no. 2, pp. 233–268, 2003. DOI: 10.4310/ATMP.2003.v7.n2.a2. arXiv: gr-qc/0304074.

[35] P. Singh, *Loop quantum cosmology and the fate of cosmological singularities*, 2015. arXiv: 1509.09182 [gr-qc].

[36] A. Ashtekar and P. Singh, "Loop Quantum Cosmology: A Status Report," *Class. Quant. Grav.*, vol. 28, p. 213001, 2011. DOI: 10.1088/0264-9381/28/21/213001. arXiv: 1108.0893 [gr-qc].

[37] K. Vandersloot, "Hamiltonian constraint of loop quantum cosmology," *Physical Review D*, vol. 71, no. 10, May 2005, ISSN: 1550-2368. DOI: 10.1103/physrevd.71.103506. [Online]. Available: http://dx.doi.org/10.1103/PhysRevD.71.103506.

[38] I. Agullo and P. Singh, *Loop quantum cosmology: A brief review*, 2016. arXiv: 1612.01236 [gr-qc].

[39] M. Bojowald, "Non-bouncing solutions in loop quantum cosmology," *Journal of Cosmology and Astroparticle Physics*, vol. 2020, no. 07, pp. 029–029, Jul. 2020. DOI: 10.1088/1475-7516/2020/07/029. [Online]. Available: https://doi.org/10.1088/1475-7516/2020/07/029.

[40] ——, "Critical evaluation of common claims in loop quantum cosmology," *Universe*, vol. 6, no. 3, p. 36, Feb. 2020, ISSN: 2218-1997. DOI: 10.3390/universe6030036. [Online]. Available: http://dx.doi.org/10.3390/universe6030036.

[41] E. Bianchi, C. Rovelli, and F. Vidotto, "Towards spinfoam cosmology," *Physical Review D*, vol. 82, no. 8, Oct. 2010, ISSN: 1550-2368. DOI: 10.1103/physrevd.82.084035. [Online]. Available: http://dx.doi.org/10.1103/PhysRevD.82.084035.

[42] F. Vidotto, "Spinfoam cosmology," *Journal of Physics: Conference Series*, vol. 314, p. 012 049, Sep. 2011, ISSN: 1742-6596. DOI: 10.1088/1742-6596/314/1/012049. [Online]. Available: http://dx.doi.org/10.1088/1742-6596/314/1/012049.

[43] W. J. Fairbairn and C. Meusburger, "Quantum deformation of two four-dimensional spin foam models," *Journal of Mathematical Physics*, vol. 53, no. 2, p. 022 501, Feb. 2012, ISSN: 1089-7658. DOI: 10.1063/1.3675898. [Online]. Available: http://dx.doi.org/10.1063/1.3675898.

[44] P. A. R. Ade, N. Aghanim, M. Arnaud, M. Ashdown, J. Aumont, C. Baccigalupi, A. J. Banday, R. B. Barreiro, J. G. Bartlett, and et al., "Planck2015 results," *Astronomy & Astrophysics*, vol. 594, A13, Sep. 2016, ISSN: 1432-0746. DOI: 10.1051/0004-6361/201525830. [Online]. Available: http://dx.doi.org/10.1051/0004-6361/201525830.

[45] E. Bianchi, M. Han, C. Rovelli, W. Wieland, E. Magliaro, and C. Perini, "Spinfoam fermions," *Classical and Quantum Gravity*, vol. 30, no. 23, p. 235 023, Oct. 2013, ISSN: 1361-6382. DOI: 10.1088/0264-9381/30/23/235023. [Online]. Available: http://dx.doi.org/10.1088/0264-9381/30/23/235023.